Atmos. Chem. Phys., 20, 2387–2405, 2020
https://doi.org/10.5194/acp-20-2387-2020
© Author(s) 2020. This work is distributed under
the Creative Commons Attribution 4.0 License.

Atmospheric Chemistry and Physics
Open Access
EGU

Long-range aerosol transport and impacts on size-resolved aerosol composition in Metro Manila, Philippines

Rachel A. Braun[1], Mojtaba Azadi Aghdam[1], Paola Angela Bañaga[2,3], Grace Betito[3], Maria Obiminda Cambaliza[2,3], Melliza Templonuevo Cruz[2,4], Genevieve Rose Lorenzo[2], Alexander B. MacDonald[1], James Bernard Simpas[2,3], Connor Stahl[1], and Armin Sorooshian[1,5]

[1]Department of Chemical and Environmental Engineering, University of Arizona, Tucson, AZ, USA
[2]Manila Observatory, Loyola Heights, Quezon City 1108, Philippines
[3]Department of Physics, School of Science and Engineering, Ateneo de Manila University, Loyola Heights, Quezon City 1108, Philippines
[4]Institute of Environmental Science and Meteorology, University of the Philippines, Diliman, Quezon City 1101, Philippines
[5]Department of Hydrology and Atmospheric Sciences, University of Arizona, Tucson, AZ, USA

Correspondence: Armin Sorooshian (armin@email.arizona.edu)

Received: 7 May 2019 – Discussion started: 30 August 2019
Revised: 24 January 2020 – Accepted: 29 January 2020 – Published: 28 February 2020

Abstract. This study analyzes long-range transport of aerosol and aerosol chemical characteristics based on instances of high- and low-aerosol-loading events determined via ground-based size-resolved aerosol measurements collected at the Manila Observatory in Metro Manila, Philippines, from July to October 2018. Multiple data sources, including models, remote sensing, and in situ measurements, are used to analyze the impacts of long-range aerosol transport on Metro Manila and the conditions at the local and synoptic scales facilitating this transport. Through the use of case studies, evidence of long-range transport of biomass burning aerosol and continental emissions is identified in Metro Manila. Long-range transport of biomass burning aerosol from the Maritime Continent, bolstered by southwesterly flow and permitted by low rainfall, was identified through model results and the presence of biomass burning tracers (e.g., K, Rb) in the ground-based measurements. The impacts of emissions transported from continental East Asia on the aerosol characteristics in Metro Manila are also identified; for one of the events analyzed, this transport was facilitated by the nearby passage of a typhoon. Changes in the aerosol size distributions, water-soluble chemical composition, and contributions of various organic aerosol species to the total water-soluble organic aerosol were examined for the different cases. The events impacted by biomass burning transport had the overall highest concentration of water-soluble organic acids, while the events impacted by long-range transport from continental East Asia showed high percent contributions from shorter-chain dicarboxylic acids (i.e., oxalate) that are often representative of photochemical and aqueous processing in the atmosphere. The low-aerosol-loading event was subject to a larger precipitation accumulation than the high-aerosol events, indicative of wet scavenging as an aerosol sink in the study region. This low-aerosol event was characterized by a larger relative contribution from supermicrometer aerosols and had a higher percent contribution from longer-chain dicarboxylic acids (i.e., maleate) to the water-soluble organic aerosol fraction, indicating the importance of both primary aerosol emissions and local emissions.

1 Introduction

Better understanding of long-range transport of aerosol is critical for determining the fate of atmospheric emissions and improving models of atmospheric aerosol. Nutrients (e.g., Duce et al., 1991; Artaxo et al., 1994), bacteria (e.g., Bovallius et al., 1978; Maki et al., 2019), and pollutants (e.g., Nordø, 1976; Lyons et al., 1978; Lindqvist et al., 1991) can be transported through the atmosphere over large distances across the globe. Atmospheric aerosol can undergo phys-

iochemical changes through photochemical and aqueous-processing mechanisms such that their characteristics at the emission source can be quite different from those farther downwind (e.g., Yokelson et al., 2009; Akagi et al., 2012). Large uncertainties remain in atmospheric aerosol models due to impacts of aqueous processing and wet scavenging on aerosol (Kristiansen et al., 2016; Xu et al., 2019).

The plethora of both natural and anthropogenic emissions in and around Southeast (SE) Asia; the proximity of islands and continental regions in SE and East Asia; and the large, growing population makes SE Asia a prime candidate for the study of long-range transport of atmospheric aerosol. Moreover, the extensive cloud coverage and precipitation during certain times of the year in SE Asia allow for an examination of the effects of aqueous processing and wet scavenging. Characterizations of aerosol in mainland SE Asia and the Maritime Continent (MC), which includes the islands south of the Philippines and north of Australia (e.g., islands part of Malaysia and Indonesia), have found major emission sources to be industrial activities, shipping, urban megacities, and biomass burning (Reid et al., 2013). In addition, natural emission sources, including marine emissions, plant life, and occasionally volcanic eruptions, intermingle with anthropogenic emissions. Mixing of aerosol from anthropogenic and biogenic sources has been noted to be influential in the overall production of secondarily produced aerosol via gas-to-particle conversion processes (Weber et al., 2007; Goldstein et al., 2009; Brito et al., 2018). In addition, the mixing of marine and biomass burning emissions can produce compositional changes, such as enhancements in chloride depletion (e.g., Braun et al., 2017) and methanesulfonate (MSA) production (Sorooshian et al., 2015). The mechanisms governing aerosol changes in mixed air masses have wide-ranging and complex impacts and require further study in regions, such as SE Asia, that are impacted by multiple aerosol emission sources.

One major contributor to atmospheric aerosol in SE Asia and the MC that has received considerable attention is biomass burning. Biomass burning in SE Asia appears to be dominated by anthropogenic activities, such as peatland burning (Graf et al., 2009; Reid et al., 2013; Latif et al., 2018) and rice straw open-field burning (Gadde et al., 2009). However, current satellite retrievals underestimate the true emissions in the region (Reid et al., 2013). Identification of biomass burning emissions in the MC using satellite-based observations is difficult for numerous reasons, including the characteristics of fires common to the region (e.g., low-temperature peat burning) and abundant cloud cover (Reid et al., 2012, 2013). However, the potential for long-range transport of biomass burning emissions from the MC has received considerable attention (Wang et al., 2013; Xian et al., 2013; Reid et al., 2016a; Atwood et al., 2017; Ge et al., 2017; Song et al., 2018). In order to better understand the frequency, amount, and fate of biomass burning emissions in the MC and SE Asia, both in situ measurements and modeling studies are needed. Insights into the fate of biomass burning emissions in the atmosphere are crucial and applicable on a global scale, especially since studies have indicated an increasing trend in biomass burning worldwide (Flannigan et al., 2009, 2013).

As a megacity in SE Asia, Metro Manila, Philippines (population in 2015 $\sim$ 12.88 million; Philippine Statistics Authority, 2020), is a prime location for the study of locally produced urban anthropogenic aerosol (Kim Oanh et al., 2006) that is mixed with biogenic, natural, and anthropogenic pollutants from upwind areas. Previous research conducted at the Manila Observatory (MO) in Quezon City, Metro Manila, characterized $PM_{2.5}$ (particulate matter, PM, with aerodynamic diameter less than 2.5 µm) and sources of measured particles, with traffic emissions being the major source at MO (Simpas et al., 2014). Interestingly, levels of measured $PM_{2.5}$ at MO showed little variance between the wet (June–October) and dry seasons (Simpas et al., 2014). Additional studies have further characterized vehicular emissions by focusing on black carbon (BC) particulate concentrations in sites around the Metro Manila region, including near roadways (Bautista et al., 2014; Kecorius et al., 2017; Alas et al., 2018). Due to very high population density in Metro Manila, it is expected that many of the urban PM sampling sites are highly affected by local anthropogenic sources as opposed to long-range transport. However, the proximity of the Philippines to other islands and continental Asia raises the question of the relative impacts of long-range transport as opposed to local emissions on not just Metro Manila but also downwind regions.

Long-range transport to the Philippines varies by season since there is a strong change in weather patterns throughout the year (Bagtasa et al., 2018). Another study of the aerosol over the South China Sea (SCS), which is bordered to the east by the Philippines, found seasonal changes in aerosol emission sources, with year-round anthropogenic pollution, smoke from the MC between August and October, and dust from northern continental Asia between February and April (Lin et al., 2007). The season from approximately June to September (Cayanan et al., 2011; Cruz et al., 2013), referred to as the Southwest Monsoon (SWM) season, is characterized by increased prevalence of southwesterly winds and precipitation. During the SWM season, biomass burning is prevalent in the MC, while biomass burning is more common in continental SE Asia during the winter and spring (Lin et al., 2009; Reid et al., 2013). While variability exists in the start dates of the different seasons, the northeast monsoon transition generally occurs in October (Cruz et al., 2013), and previous research has defined this season as occurring from October to February (Bagtasa, 2011). During the northeast monsoon, aerosol influences from northern East Asia were measured in the northwestern edge of the Philippines (Bagtasa et al., 2018). In addition to transport of aerosol to the Philippines, the influence of emission outflows from the Philippines has also been measured in the northern SCS at

Dongsha Island (Chuang et al., 2013) and in coastal southeast China (Zhang et al., 2012). Long-range transported aerosol in SE and East Asia has various sources and, therefore, different physiochemical properties. However, the prevalence of the signal of long-range transported aerosol in a highly polluted megacity, such as Metro Manila, is not well characterized.

As recent studies have indicated a decline in SWM rainfall in the western Philippines and an increase in no-rain days during the typical SWM season (Cruz et al., 2013), the potential for wet scavenging of aerosol during these time periods could be decreasing. Furthermore, decreases in monsoonal rainfall in other parts of Asia, including India (Dave et al., 2017) and China (Liu et al., 2019), have been linked to increases in aerosol, especially those of anthropogenic origin. Reinforcing mechanisms in these interactions, such as decreased rainfall reducing wet scavenging, leading to higher aerosol concentrations that in turn suppress precipitation, and the corresponding climatic changes in monsoonal rain in the western Philippines underscore the need to better understand the processes governing atmospheric aerosol characteristics and sources, especially during the monsoonal season.

The present study focuses on three high-aerosol-loading events, contrasted with a very low aerosol event, as identified by ground-based observations collected at MO from July to October 2018. The objectives of the study are to (i) describe synoptic- and local-scale conditions facilitating various transport cases; (ii) characterize aerosol physicochemical properties associated with long-range transport; and (iii) identify transformational processes, especially with regard to chemical composition, of aerosol during long-range transport to the highly populated Metro Manila region. The results of this work have implications for better understanding (i) the fate of biomass burning emissions in a region with prevalent wildfires that are poorly characterized by remote sensing; (ii) the impact of transformational and removal mechanisms, including aqueous processing, photochemical reactions, and wet scavenging, on long-range transported aerosol from multiple sources; and (iii) typical synoptic- and local-scale behavior of aerosol in a region that is both highly populated and gaining increasing attention due to campaigns such as the NASA-sponsored Clouds, Aerosols, and Monsoon Processes Philippines Experiment ($CAMP^2Ex$).

2 Methodology

2.1 Ground-based observations

As part of a year-long sampling campaign ($CAMP^2Ex$ weatHEr and CompoSition Monitoring: CHECSM) at the Manila Observatory (MO; 14.64° N, 121.08° E) in Quezon City, Metro Manila, Philippines, 12 sets of size-resolved aerosol were collected from July to October 2018 using a micro-orifice uniform deposit impactor (MOUDI; Marple et al., 2014). Details for the 12 size-resolved sets can be found in Table 1. Sample Teflon substrates (PTFE membrane, 2 µm pore, 46.2 mm diameter, Whatman) were cut in half for preservation for future analysis. Half-substrates were extracted in 8 mL of Milli-Q water (18.2 MΩ cm) in sealed polypropylene vials through sonication for 30 min. Aqueous extracts were subsequently analyzed for ions using ion chromatography (IC; Thermo Scientific Dionex ICS-2100 system) and elements using triple quadrupole inductively coupled plasma mass spectrometry (ICP-QQQ; Agilent 8800 Series). The list of analyzed species and limits of detection for those species can be found in Table S1 in the Supplement, with limits of detection in the parts per trillion (ppt) range for ICP and the parts per billion (ppb) range for IC. Background concentrations were also subtracted from each sample. For each MOUDI set (naming convention: MO#), the mass concentration sum of the water-soluble species was calculated; using this summation, the three high-aerosol-loading events were identified (MO7, MO12, and MO14), as well as the lowest aerosol event (MO11). The average ± standard deviation of the total water-soluble species measured for the remaining eight sets not identified in the high or low categories is 6.99 ± 2.71 µg m^{-3}.

2.2 Remote-sensing observations

Retrievals of atmospheric profiles from the Cloud-Aerosol Lidar with Orthogonal Polarization (CALIOP) on board the Cloud-Aerosol Lidar and Infrared Pathfinder Satellite Observation (CALIPSO) satellite were taken for select satellite overpasses corresponding to MOUDI sample sets of interest (Winker et al., 2009). Previous studies have examined the ability of CALIOP to capture atmospheric profiles in SE Asia and the MC, with one major challenge in this region being the lack of cloud-free schemes (Campbell et al., 2013; Ross et al., 2018). Overpasses corresponding to the three highest aerosol events were analyzed, but no data were available for the time encompassing MO11. The CALIOP Level 2 Vertical Feature Mask (VFM) version 4.20 was used to distinguish between clear air, clouds, and aerosol (Vaughan et al., 2004). For figures of CALIOP VFM data in this study, data are plotted at 30 m vertical resolution every 5 km along the satellite ground track.

2.3 Models

To describe the synoptic-scale conditions, data were used from the Modern-Era Retrospective analysis for Research and Applications, version 2 (MERRA-2; Gelaro et al., 2017). Horizontal winds at 850 hPa (GMAO, 2015a) were temporally averaged over the sampling period using 3 h instantaneous data and subsequently spatially averaged to increase figure readability. The total cloud area fraction (GMAO, 2015b) was also temporally averaged over the sampling period using 1 h time-averaged MERRA-2 data.

Table 1. Description of the MOUDI sample sets from this study. Accumulated precipitation during the sample sets was found using PERSIANN-CCS for the area bounded by 14.6067–14.6946° N and 121.0199–121.0968° E.

Set name	Start date (MM/DD/YY)/ local time	End date/ local time	Total water-soluble species ($\mu g\,m^{-3}$)	% of water-soluble mass $< 1\,\mu m$	Precipitation (mm)
MO1	7/19/18 12:40	7/20/18 12:43	4.61	67.3 %	27
MO2	7/23/18 11:29	7/25/18 17:10	6.52	62.1 %	14
MO4	7/25/18 19:16	7/30/18 18:12	5.17	66.4 %	35
MO5	7/30/18 19:17	8/1/18 13:19	9.17	64.8 %	11
MO6	8/6/18 14:33	8/8/18 14:38	5.11	55.8 %	50
MO7	8/14/18 13:59	8/16/18 14:04	13.70	60.3 %	3
MO8	8/22/18 13:46	8/24/18 13:53	12.73	71.6 %	10
MO9	9/1/18 05:00	9/3/18 05:05	6.23	76.7 %	64
MO10	9/10/18 14:42	9/12/18 15:02	6.36	79.5 %	20
MO11	9/18/18 14:12	9/20/18 14:24	2.70	47.3 %	26
MO12	9/26/18 13:53	9/28/18 13:53	13.49	59.9 %	1
MO14	10/6/18 05:00	10/8/18 05:05	16.55	78.4 %	0

Five-day air mass back trajectories were calculated using the Hybrid Single Particle Lagrangian Integrated Trajectory (HYSPLIT) model from NOAA (Stein et al., 2015) and gridded meteorological data from the National Centers for Environmental Prediction/National Center for Atmospheric Research (NCEP/NCAR) reanalysis project. The model was run for back trajectories terminating at the MOUDI inlet (~ 85 m above sea level) starting at the beginning of the sample set and every 6 h thereafter during each sample set, resulting in $(1 + N/6)$ trajectories for each set, where N is the total number of sampling hours. Heights above ground level for HYSPLIT back trajectories corresponding to the three high-aerosol-loading events (MO7, MO12, and MO14) can be found in Fig. S1 in the Supplement. The HYSPLIT model has been used extensively in studies focused on regions across the globe to study aerosol transport (Stein et al., 2015).

Precipitation amounts were found using the Precipitation Estimation from Remotely Sensed Information using Artificial Neural Networks–Cloud Classification System (PERSIANN-CCS) dataset (Hong et al., 2004), which is available from the UC Irvine Center for Hydrometeorology and Remote Sensing (CHRS) Data Portal (Nguyen et al., 2019). PERSIANN-CCS has previously been used to analyze precipitation events in the region of interest, as shown by the successful characterization of rainfall during Typhoon Haiyan over the Philippines in November 2013 (Nguyen et al., 2014). Benefits of PERSIANN-CCS include the data availability at $0.04° \times 0.04°$ spatial resolution, while uncertainties in the dataset arise from sources such as a lack of bias correction (Nguyen et al., 2014). Precipitation accumulated during the sample sets (Table 1) was calculated to be the average found for the region surrounding MO in the box bounded by 14.6067–14.6946° N and 121.0199–121.0968° E.

To further describe long-range transport activity, results from the Navy Aerosol Analysis and Prediction System (NAAPS) operational model are included for the selected

study periods (Lynch et al., 2016; https://www.nrlmry.navy.mil/aerosol/, last access: 20 February 2019). Global meteorological fields used in the NAAPS model are supplied by the Navy Global Environmental Model (NAVGEM; Hogan et al., 2014). The NAAPS model has previously been employed to study aerosol in the MC (e.g., Xian et al., 2013).

3 Results

3.1 Cases of long-range aerosol transport

The following sections (3.1.1–3.1.4) describe the synoptic- and local-scale meteorological conditions governing long-range aerosol transport during the three highest aerosol events (MO7, MO12, and MO14) and, for the purposes of comparison, the lowest aerosol event (MO11). Also included are characterizations of aerosol from remote-sensing and model results. Results of size-resolved aerosol characterization at MO are discussed in Sect. 3.2.

3.1.1 MO7 (14–16 August 2018): smoke transport from the Maritime Continent

Many previous studies have focused on the prevalence of biomass burning in the MC and the potential for transport of smoke towards the Philippines (Wang et al., 2013; Xian et al., 2013; Reid et al., 2016a; Atwood et al., 2017; Ge et al., 2017; Song et al., 2018). Figure 1a shows the average 850 hPa wind vectors and cloud fraction for the MO7 sampling period. The prevailing wind direction was towards the northeast, consistent with typical SWM flow. Furthermore, areas with lower cloud coverage were present to the southwest of Metro Manila. The HYSPLIT back trajectory for this sample set also shows an air mass originating around the MC to the southwest of MO that is then transported over the ocean towards the Philippines (Fig. 2a). As evidenced by the name of the season (i.e., Southwest Monsoon), this trajectory is typical for this time of the year and was the dominating trajectory pattern for the remaining eight sample sets not chosen for in-depth analysis (Fig. S2). Furthermore, for MO1–MO10 (i.e., all sample sets with prevailing southwesterly wind influence), MO7 had the lowest rain amount for the surrounding region, followed by MO8, which had the fourth-highest water-soluble aerosol concentration (Table 1). This suggests that wet scavenging could have been less influential in MO7 and MO8, thereby leading to an increase in the PM measured. Three CALIPSO overpasses near MO occurred during the MO7 sample set and one occurred during the nighttime after sampling ended; however, the signal was largely attenuated in the lower 8 km during the daytime samples for the area surrounding MO (Fig. S3). In the case of the two nighttime overpasses (Fig. 3), which sampled to the southwest of Manila, a deep aerosol layer is observed in the VFM extending from the surface to around 3 km (Fig. 3). This classic case of long-range transport from the MC to the Philippines during the SWM season is also clearly shown in the biomass burning smoke surface concentrations from the NAAPS model (Fig. 4a).

3.1.2 MO11 (18–20 September 2018): lowest aerosol event

MO11 had the lowest overall water-soluble aerosol mass concentration (2.7 $\mu g\,m^{-3}$), which is over 6 times lower than the highest aerosol MOUDI set. As evidenced by both the 850 hPa wind vectors (Fig. 1b) and the HYSPLIT back trajectories (Fig. 2b) from this set, conditions are very different from the highest three aerosol events and show transport patterns with flow originating over the open ocean to the east of the Philippines moving almost due west. The lack of anthropogenic aerosol sources in the path of the back trajectories could result in the overall low amount of aerosol observed. This set was also characterized by high accumulated rainfall amounts for the region in the path of the back trajectories (Fig. 2b) and in the area surrounding MO as compared to the highest aerosol events (Table 1), increasing the possibility that wet scavenging effectively removed most of the transported (and, to some extent, local) aerosol. In addition, the NAAPS model showed no smoke influence from the MC and an isolated anthropogenic and biogenic fine aerosol plume around Metro Manila, suggesting local sources accounted for the majority of the measured aerosol (Fig. 4b).

3.1.3 MO12 (26–28 September 2018): impacts of Typhoon Trami

Typhoon Trami (Category 5) passed to the northeast of the island of Luzon in the Philippines during MO12 (Fig. 1c). Typhoon influences on atmospheric aerosol, caused by varying factors such as wind speed and precipitation, have been studied in China (Yan et al., 2016; Liu et al., 2018), Korea (Kim et al., 2007), Malaysia (Juneng et al., 2011), the South China Sea (Reid et al., 2015, 2016b), and Taiwan (Fang et al., 2009; Chang et al., 2011; Lu et al., 2017). The influences of typhoons on biomass burning emissions and transport in the MC have also been examined (Reid et al., 2012; Wang et al., 2013). In this case, the influence of this storm changed the prevailing wind direction approaching the northern Philippines, effectively pulling an air mass from the west of the island and, along with it, emissions from continental East Asia (Fig. 2c). Furthermore, the air mass passed through regions of relatively little rainfall during transport to the Philippines (Fig. 2c), and accumulated rainfall at MO during this sample set was very low (Table 1). One CALIPSO overpass around the ending time of set MO12 and one during the nighttime after sampling ended (Fig. 3) show that, in the direction of transport (i.e., north of the MO, from around 15–20° N), there is an aerosol layer extending up to around 2 km during the day (northwest of MO) and 3 km at night (northeast of MO). The influence of emissions from continental East

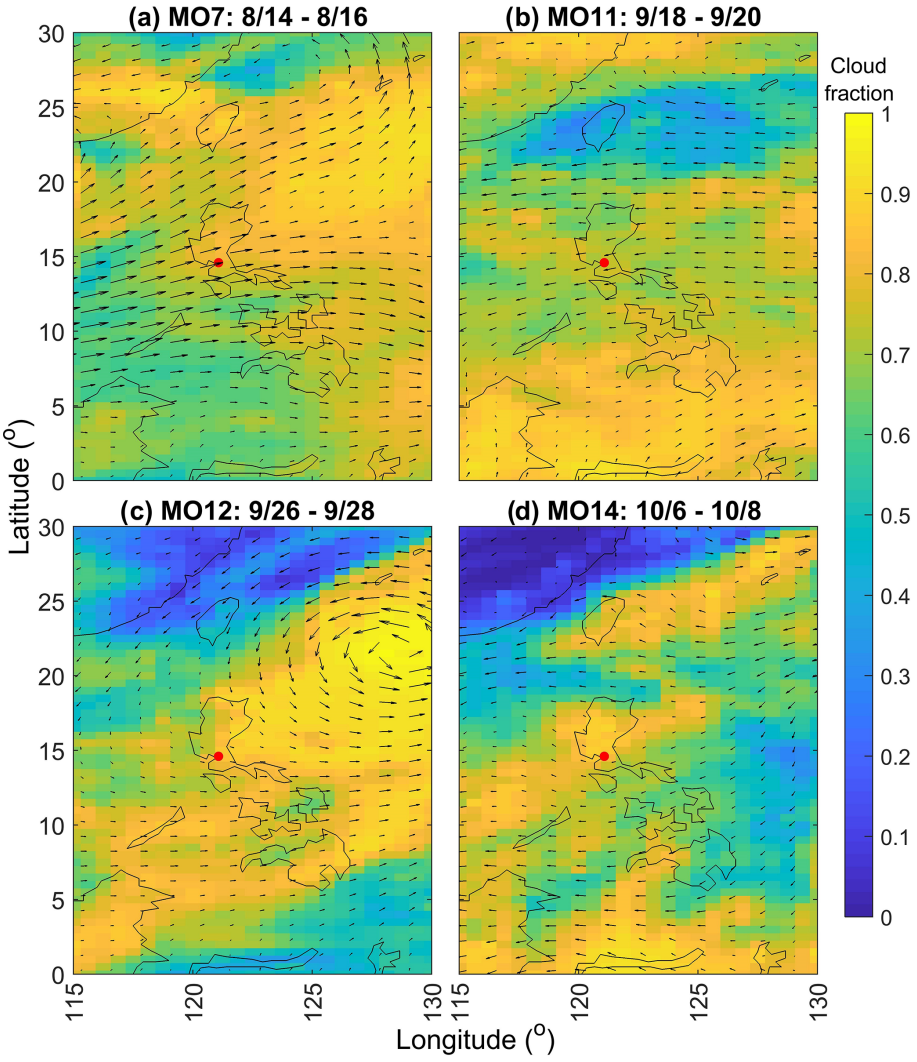

Figure 1. MERRA-2 data for 850 hPa wind vectors and total cloud fraction averaged over the sample set duration for **(a)** MO7 (14–16 August), **(b)** MO11 (18–20 September), **(c)** MO12 (26–28 September), and **(d)** MO14 (6–8 October). The location of the Manila Observatory is indicated by the red circle. (Note that 850 hPa wind vectors are also averaged to increase grid spacing and improve figure readability.)

Asia is also apparent in the NAAPS model (Fig. 4c). Observations at Dongsha Island, located to the north of the Philippines, have revealed influence from Gobi Desert emissions (Wang et al., 2011) and anthropogenic sources (Atwood et al., 2013). Farther south in the MC, aerosol measurements in Malaysia have also indicated influence of aged, long-range transport from sites to the north in East Asia (Farren et al., 2019).

3.1.4 MO14 (6–8 October 2018): mixed influences

The final MOUDI set (MO14) included in this study represents a transition in meteorological regimes at the end of the SWM season and resulted in the highest overall water-soluble mass concentration. This event had some of the lowest rainfall amounts in the region surrounding Metro Manila (Fig. 2d), with zero accumulated precipitation at MO during the sampling period (Table 1). Furthermore, low cloud fraction was observed for regions to the northwest and east of Metro Manila (Fig. 1d). Back trajectories from HYSPLIT show that the air mass appeared to be influenced by a mix of continental sources in East Asia and local sources (Fig. 2d). Furthermore, two CALIPSO overpasses, one during the nighttime while sampling was occurring and the other during the daytime after sampling ended, show a deep aerosol layer north of MO, extending from the surface to around 2 km on 6 October and lower on 8 October (Fig. 3). From the NAAPS model, it appears that a mixture of MC smoke emissions and continental East Asia emissions converges around the northern Philippines (Fig. 4d).

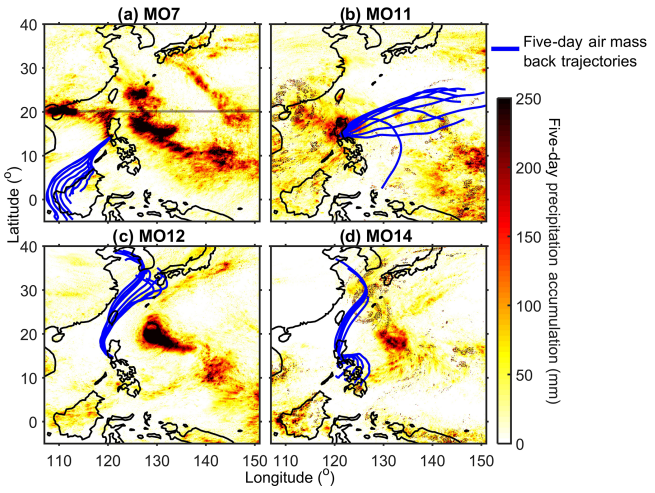

Figure 2. Rainfall accumulation, extending from 5 d before the midpoint of each sample set until the midpoint of each sample set, from PERSIAN-CCS for **(a)** MO7, **(b)** MO11, **(c)** MO12, and **(d)** MO14. In blue are the 5 d air mass back trajectories terminating at the MOUDI inlet at MO (∼ 85 m above sea level) every 6 h during each of the sample study periods. Note that the maximum precipitation accumulation in the region shown during the study periods was 955 mm; however, for figure readability, the scale was reduced to 0–250 mm.

3.2 Ground-based aerosol chemical composition

3.2.1 Size-resolved aerosol characteristics

The water-soluble mass size distributions and the percent contribution of each MOUDI stage to the water-soluble mass for the four sets of interest (MO7, MO12, MO14, and MO11) and the average (± 1 standard deviation) of the remaining sets (MO1–MO6, MO8–MO10) are shown in Fig. 5. Most of the sets show a bimodal distribution with peaks in both the submicrometer and supermicrometer range; one exception is the lowest aerosol event (MO11), which shows a fairly broad size distribution. The highest aerosol event, MO14, shows a significant peak in the submicrometer range, with a very large drop in mass concentration in the supermicrometer range. This is in stark contrast to the lowest aerosol event (MO11), which shows that the supermicrometer range contributes the greatest percent to the total water-soluble mass. The second- and third-highest aerosol events, MO7 and MO12, also show significant enhancements in the supermicrometer range as compared to the average of the other sets and MO14.

Figure 6 describes the major species contributing to the water-soluble mass. MO14 had one of the highest combined contributions of SO_4^{2-} and NH_4^+ (77.2 % of water-soluble mass), with only MO10 being slightly larger at 77.6 %. These two species are typically associated with the submicrometer range and anthropogenic origins due to their formation through secondary processes such as gas-to-particle conversion of gaseous SO_2 and NH_3, respectively, and aqueous processing to form SO_4^{2-} (Ervens, 2015). In contrast, MO11 had the lowest overall combined percent contribution of these two species (41.4 %) to the water-soluble aerosol mass. Of all 12 SWM MOUDI sets, MO11 had the highest percent contributions from Ca^{2+} (14.0 %) and Cl^- (12.5 %), as well as one of the highest contributions from Na^+ (10.7 %). Each of these species is associated with primary emissions, including dust in the case of Ca^{2+} and sea salt for Na^+ and Cl^-, resulting in larger particles (i.e., > 1 µm). The HYSPLIT back trajectories for MO11 match well with the MOUDI results, as the influence of marine aerosol (i.e., Na^+, Cl^-) and lack of anthropogenic sources of SO_2 and NH_3 are apparent. Local sources of dust most likely contribute the highest amount to the measured Ca^{2+}, as the back trajectories show few other crustal sources farther upwind. Average size-resolved profiles for all of the species in these 12 sample sets can be found in Cruz et al. (2019), with characteristic size distribution profiles agreeing with the above assessments.

3.2.2 Enhancements in tracer species

In addition to insights from the major water-soluble chemical species found in aerosol, tracer aerosol species can also be used to identify impacting emission sources (e.g., Fung and Wong, 1995; Allen et al., 2001; Ma et al., 2019). For the aforementioned high-aerosol events, numerous tracer species are elevated in some, but not all, sample sets. This makes these species prime candidates for linking influencing sources to the measured ambient aerosol. The authors theorize that MO8, which was the fourth-highest aerosol event (Table 1), also was impacted by biomass burning due to the back-trajectory analysis (Fig. S2), NAAPS model (Fig. S4), and increases in select species described subsequently. Therefore, MO8 was separated from the other sample sets for the purposes of the following characterizations. Figure 7 shows the size-resolved aerosol composition for select tracer species for the four highest aerosol events (MO7, MO8, MO12, and MO14), the lowest aerosol event (MO11), and the average (± standard deviation) of the remaining seven sample sets.

Potassium is frequently used as a biomass burning tracer (e.g., Andreae, 1983; Artaxo et al., 1994; Echalar et al., 1995; Chow et al., 2004; Thepnuan et al., 2019). This species shows highly elevated levels in the submicrometer range for MO7 and MO8 (i.e., the sets influenced by biomass burning transport from the MC). Other elevated trace elements for these two profiles include Rb, Cs, Se, and Ti (Fig. 7). Previous studies in the western United States (Schlosser et al., 2017; Ma et al., 2019) have also shown Rb enhancements in wildfire-influenced aerosol. Rb has also been measured in flaming and smoldering biomass burning emissions (Yamasoe et al., 2000). Enhancements in Rb and Cs in the fine fraction of aerosol influenced by wildfire emissions have been observed in South Africa (Maenhaut et al., 1996), with

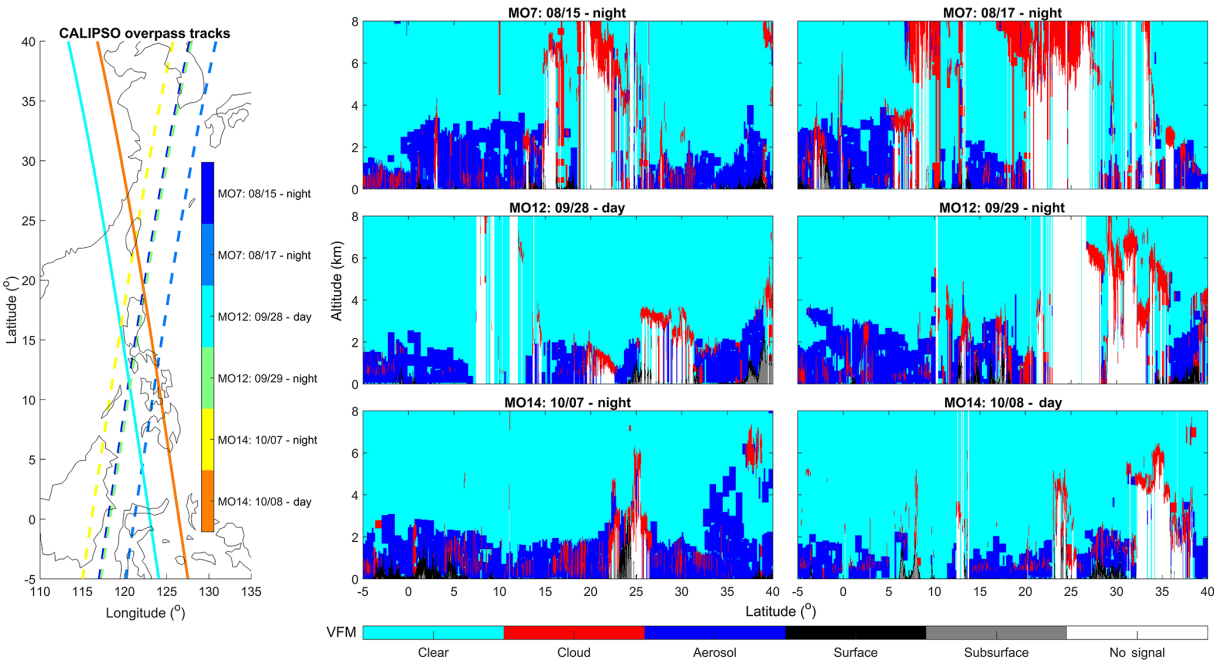

Figure 3. CALIOP Vertical Feature Mask (VFM) for overpasses during or following MO7, MO12, and MO14. For the CALIPSO satellite overpass tracks, the dashed lines correspond to the nighttime profiles and solid lines are for daytime. Note that nighttime overpasses correspond to early morning times before sunrise for the listed days and daytime overpasses occurred during the early afternoon.

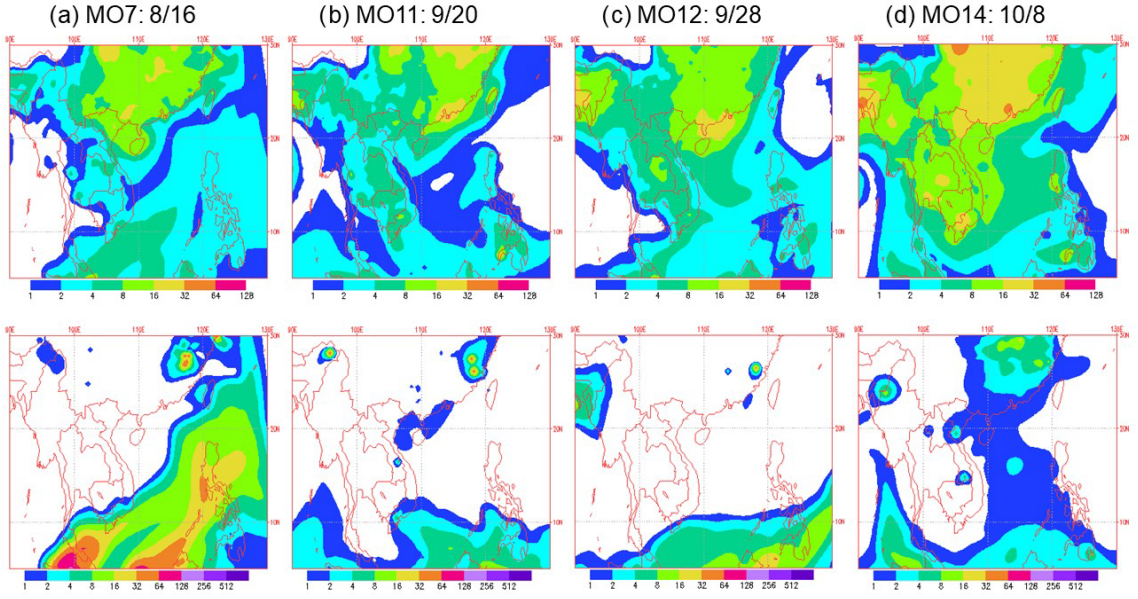

Figure 4. NAAPS model snapshots corresponding to conditions at the stop time of sample sets **(a)** MO7, **(b)** MO11, and **(c)** MO12 and **(d)** 3 h after the sample stop time for MO14. The top row of figures is anthropogenic and biogenic fine aerosol (ABF) surface concentration ($\mu g\,m^{-3}$), while the bottom row is biomass burning smoke surface concentration ($\mu g\,m^{-3}$).

similar results shown in this study for aerosol in the submicrometer size range. Se is also enhanced for these two sets in the submicrometer range, as it is often formed through gas-to-particle conversion processes of inorganic Se compounds (Wen and Carignan, 2007). A wide variety of sources for atmospheric Se exist (Mosher and Duce, 1987), including, but not limited to, coal combustion (Thurston and Spengler, 1985; Fung and Wong, 1995; Song et al., 2001), marine emissions (Arimoto et al., 1995), volcanos, and biomass burning (Mosher and Duce, 1987). In contrast to the other en-

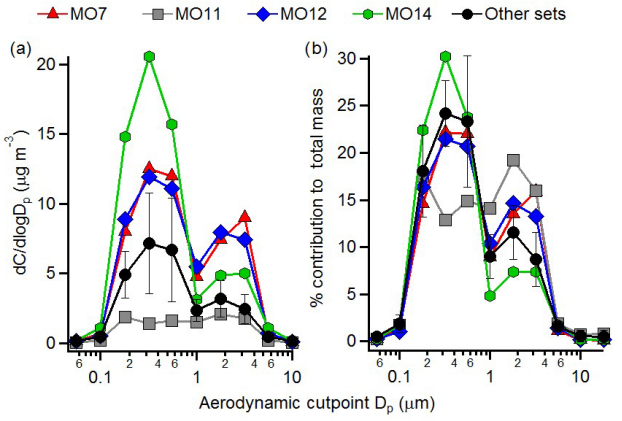

Figure 5. **(a)** Mass size distributions for total water-soluble mass (C is the sum of mass concentrations for water-soluble species) and **(b)** percent contribution of each size range to the total water-soluble mass for the three MOUDI sets with the highest aerosol mass concentrations (MO7, MO12, and MO14), the set with the lowest concentration (MO11), and the average (± 1 standard deviation error bars) for the remaining eight sets.

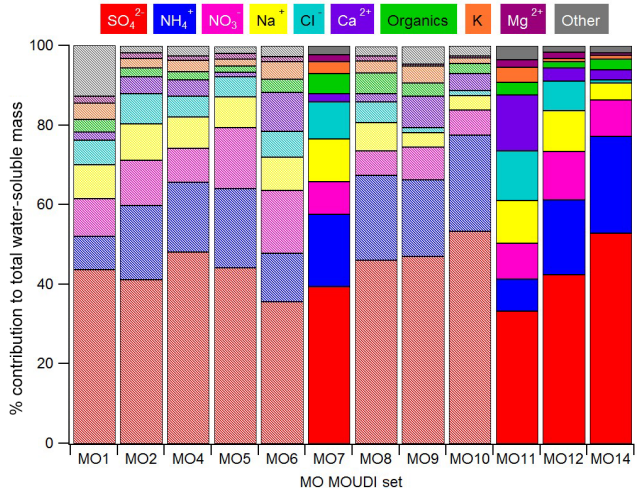

Figure 6. Percent contribution of various species to the total water-soluble mass concentration for each of the 12 sample sets. The sample sets with the three highest aerosol concentrations (MO7, MO12, and MO14) and the lowest aerosol concentration (MO11) are shown as solid bars while all other sample sets are stripes. The "organics" category contains the sum of methanesulfonate (MSA), pyruvate, adipate, succinate, maleate, oxalate, and phthalate.

hanced species for MO7 and MO8, the mass concentration mode for Ti resides in the supermicrometer size range. Ti is typically associated with crustal material that can be suspended through mechanisms such as vehicle usage (Sternbeck et al., 2002; Querol et al., 2008; Amato et al., 2009) and lofting in wildfire plumes (Maudlin et al., 2015; Schlosser et al., 2017). While long-range transport of biomass burning aerosol could lead to the enhancements measured for these

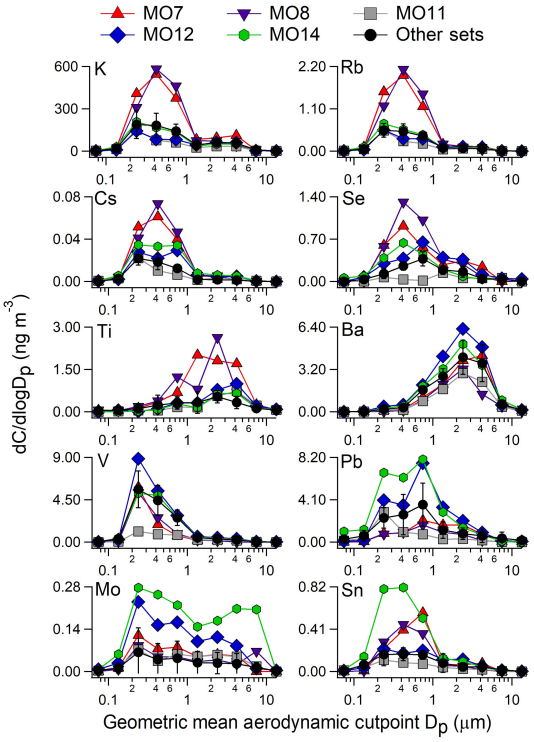

Figure 7. Selected elements that showed elevated concentrations during at least one of the highest aerosol events (MO7, MO8, MO12, or MO14). The concentrations from the lowest aerosol event (MO11) are also shown. The "other sets" category displays the average (± 1 standard deviation) for the remaining seven sets.

biomass burning tracer species, local emission sources, such as waste burning and wood burning for cooking, may also play a role.

Two tracer species are included that showed enhancements for MO12, specifically Ba in the supermicrometer range and V in the submicrometer range (Fig. 7). One well-documented source of aerosol Ba is nonexhaust vehicle emissions, including brake wear (Sternbeck et al., 2002; Querol et al., 2008; Amato et al., 2009; Jeong et al., 2019). V also has well-characterized emission sources, most specifically fuel combustion (Fung and Wong, 1995; Artaxo et al., 1999; Song et al., 2001; Lin et al., 2005; Kim and Hopke, 2008). In coastal environments, V is often tied to shipping emissions (Agrawal et al., 2008; Pandolfi et al., 2011; Maudlin et al., 2015; Mamoudou et al., 2018). As these sources are anthropogenic in origin, it is difficult to determine the relative influences of long-range transport versus local emissions, especially with the proximity of the sampling site to major roadways and shipping in Manila Bay. However, the enhancement in V could result from the transport of the aerosol over major shipping lanes farther upwind.

Finally, Fig. 7 shows three selected elements that appear enhanced in MO14, all of which are typically tied to anthropogenic sources. Both Pb and Sn are found mainly in

the submicrometer range and have been linked by previous studies to vehicle emissions (Singh et al., 2002; Amato et al., 2009), industrial emissions (Querol et al., 2008; Allen et al., 2001), and waste burning (Kumar et al., 2015). Other sources of Pb could include e-waste recycling (Fujimori et al., 2012) and biomass burning (Maenhaut et al., 1996). The size distribution of Mo for MO14 shows a much broader distribution, with peaks in both the sub- and supermicrometer ranges. Sources of Mo include vehicle emissions (Pakkanen et al., 2003; Amato et al., 2009), combustion (Pakkanen et al., 2001, 2003), and industrial activity, including copper smelters (Artaxo et al., 1999). As is the case with the enhanced species in MO12, the anthropogenic nature of these species makes it difficult to determine the relative contribution of long-range versus local emissions. However, as both MO12 and MO14 show enhancements in anthropogenically produced trace elements, the influence of long-range transport from industrial and urban areas in continental East Asia is plausible.

3.2.3 Variability of water-soluble organic species

Figure 8 shows the sum of the total measured water-soluble organic species and the relative contributions of oxalate, succinate, adipate, maleate, pyruvate, MSA, and phthalate to the total measured water-soluble organics for MO7, MO8, MO11, MO12, MO14, and the average (± 1 standard deviation) of the remaining sets. Malonate (C3) was not characterized due to its low concentrations in the samples measured and the coelution of C3 with carbonate in the IC analysis. Glutarate (C5) was also excluded from the analysis due to very low concentrations. For the examination of the organic species, MO8 was again separated from the other MOUDI sets due to it having the second-highest concentration of organic species (0.66 µg m^{-3}) and an organic species contribution profile very similar to that of MO7. The remaining MOUDI sets included in the average category (MO1–MO6, MO9–MO10) all have total organic species concentrations that were lower than the four highest aerosol sets (MO7, MO8, MO12, MO14) and greater than the lowest aerosol set (MO11). The lowest aerosol event (MO11) has the lowest overall concentration of organic aerosol (0.09 µg m^{-3}), while the second-highest aerosol event (MO7) has the highest concentration of organic aerosol (0.70 µg m^{-3}).

Many studies worldwide have examined the relative contributions of organic species to atmospheric aerosol, with oxalate typically having the highest contribution among dicarboxylic acids (Kawamura and Kaplan, 1987; Kawamura and Ikushima, 1993; Kawamura and Sakaguchi, 1999; Sorooshian et al., 2007a; Hsieh et al., 2007, 2008; Aggarwal and Kawamura, 2008; Deshmukh et al., 2012, 2018; Li et al., 2015; Hoque et al., 2017; Kunwar et al., 2019). Oxalate was the dominant water-soluble organic species for all 12 MOUDI sets, with oxalate having the highest contribution to the organic aerosol in MO12 (88.7 % of total

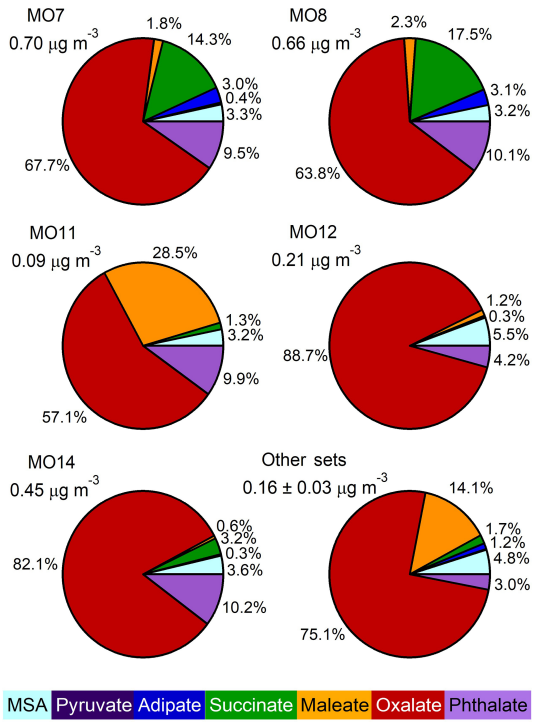

Figure 8. Pie charts showing the fraction of species contributing to the measured water-soluble organic aerosol. Below each pie chart title is the sum of the water-soluble organic species measured, with the "other sets" chart showing the average ± 1 standard deviation for the remaining sets.

organic aerosol). Oxalate is often considered a byproduct of photochemical aging of longer-chain dicarboxylic acids (e.g., Kawamura and Ikushima, 1993; Kawamura and Sakaguchi, 1999), and therefore an increase in oxalate is often considered a signature of aged aerosol in the absence of primary oxalate emissions from sources such as biomass burning. Another major pathway of oxalate formation is aqueous processing (Crahan et al., 2004; Ervens et al., 2004, 2018; Sorooshian et al., 2006, 2007b; Wonaschuetz et al., 2012), which is likely prevalent during the SWM when there is frequent cloud cover. Previous studies have also demonstrated the ability for transport and photochemical aging of water-soluble organic acids over long distances in a marine environment (e.g., Kawamura and Sakaguchi, 1999) and the importance of emissions from continental Asia in the organic aerosol budget in the western north Pacific (Aggarwal and Kawamura, 2008; Hoque et al., 2017). The back trajectories of the air masses terminating at MO during MO12 and MO14 indicate origins of emissions from continental East Asia (Fig. 2). It is plausible that the high contribution of oxalate to the organic aerosol in MO12 and MO14 (which had the fourth-highest percent contribution of oxalate) is due to the degradation of both primarily emitted and secondarily produced longer-chain dicarboxylic acids during the transport process through mechanisms described above, such

as photochemical degradation and aqueous processing, with the former mechanism being plausible in the regions of low cloud cover to the north and northwest of Manila (Fig. 1) and the latter mechanism potentially being of great importance due to the typhoon influences during transport. While the aerosol measured in MO7 and MO8 also shows long-range transport influences (Figs. 2a and S2), the overall signal of organic aerosol is much stronger in these two sets, such that the absolute concentration of oxalate (MO7: 0.47 $\mu g\,m^{-3}$; MO8: 0.42 $\mu g\,m^{-3}$) is still greater than in MO12 (0.19 $\mu g\,m^{-3}$) and MO14 (0.37 $\mu g\,m^{-3}$). However, biomass burning is a well-documented source of both oxalate and longer-chain dicarboxylic acids (e.g., Falkovich et al., 2005; Nirmalkar et al., 2015; Cheng et al., 2017; Deshmukh et al., 2018; Thepnuan et al., 2019).

Succinate has been linked to biomass burning emissions (Wang and Shooter, 2004; Falkovich et al., 2005; Zhao et al., 2014; Balla et al., 2018), vehicular emissions (Kawamura and Kaplan, 1987; Kawamura et al., 1996; Yao et al., 2004), and secondary production via photochemical reactions of precursor organic compounds (Kawamura and Ikushima, 1993; Kawamura et al., 1996; Kawamura and Sakaguchi, 1999). The two MO MOUDI sets thought to have the most influence from biomass burning emissions (MO7 and MO8) had the highest organic aerosol mass concentrations and the highest mass percent contributions of succinate to the organic aerosol (MO7: 14.3 % and MO8: 17.5 %). In contrast, the next highest contribution of succinate to the organic aerosol was 4.2 % measured in MO5. These results agree with previous studies in Northeast China that showed an increase in total organic aerosol mass concentration and a strong increase (decrease) in the relative contribution of succinate (oxalate) during biomass burning periods as opposed to non-biomass-burning periods (Cao et al., 2017). Results from California, USA, also showed higher percent contributions of succinate to the water-soluble organic aerosol during periods influenced by biomass burning (Maudlin et al., 2015).

MO11 had the second-highest relative contribution of maleate (28.5 % of water-soluble organic aerosol) out of all 12 sample sets and had a much higher percent contribution as compared to the four highest aerosol events (< 2.5 % for each of the following: MO7, MO8, MO12, and MO14). Maleate is linked to the oxidation of aromatic hydrocarbons, usually from anthropogenic sources such as vehicular emissions (Kawamura and Kaplan, 1987; Kunwar et al., 2019). One explanation for this result could be the higher rainfall accumulation in and around the study region during MO11 as compared to the three highest aerosol sets (Fig. 2). Wet scavenging could have removed aerosol from transported air masses during their journey towards MO, thereby increasing the relative contribution of local sources to the measured aerosol in MO11. Because of the reduced aging time associated with emissions from local sources, the relative increase in the contribution of longer-chain dicarboxylic acids and the decrease in the relative contribution of oxalate is plausible. Hsieh et al. (2008) showed in samples from Taiwan that the relative contribution of oxalate to the organic acids was also higher during periods of high aerosol loading as opposed to periods of moderate aerosol loading when the overall PM concentration was lower. MO11, which showed air mass back trajectories originating to the east of the Philippines from the open Pacific (Fig. 2b), had the lowest overall water-soluble PM concentration, the lowest overall concentration of water-soluble organic acids, and the second-lowest percent contribution of oxalate to the organic acid mass (57.1 %) of all the sets.

Phthalate is an aromatic dicarboxylic acid often linked to anthropogenic sources through photochemical transformation of emissions from vehicles (Kawamura and Kaplan, 1987; Kawamura and Ikushima, 1993) and waste burning (Kumar et al., 2015), although aqueous processing has also been proposed as a formation mechanism (Kunwar et al., 2019). Accordingly, phthalate has been shown to have seasonal and diurnal variations in concentration, with enhanced production usually linked to times of stronger solar radiation (i.e., summertime and daytime: Satsumabayashi et al., 1990; Ray and McDow, 2005; Ho et al., 2006; Kunwar et al., 2019). However, increased emissions of precursor species during different times of the year may affect these trends (Hyder et al., 2012). Sets MO7, MO8, MO11, and MO14 had the highest contribution to the water-soluble organics from phthalate (range: 9.5 %–10.2 %). In contrast, the remaining sets had a much lower contribution (range: 1.7 %–4.9 %). However, the absolute concentration of phthalate was highest in sets MO7, MO8, and MO14 (range: 45.3–67.0 $ng\,m^{-3}$) and much lower for the remaining sets (range: 2.0–8.9 $ng\,m^{-3}$). Increased phthalate concentrations during biomass burning episodes have been previously measured in SE Asia (Cao et al., 2017). Furthermore, cloud coverage was fairly low during MO14 as compared to the other sets of interest (Fig. 1), increasing the possibility of photochemical production of phthalate. For the remaining sample sets, the range of phthalate concentrations is substantially lower and fairly consistent, indicating that the measured phthalate in these samples most likely represents the local background conditions.

While not a carboxylic acid, MSA is nonetheless an important organic aerosol species, especially in marine environments. The assumed precursor of MSA in this study is from the oxidation of marine-emitted dimethylsulfide (DMS). Interestingly, all sample sets showed approximately the same mass percent contribution of MSA to the organic aerosol, ranging from a minimum of 3.1 % (MO6) to a maximum of 7.0 % (MO5). However, the absolute concentration of MSA was highest in the two sets with biomass burning influence (MO7: 23.3 and MO8: 21.4 $ng\,m^{-3}$), with concentrations 8.4 and 7.7 times higher, respectively, than the lowest MSA concentration measured (MO11: 2.8 $ng\,m^{-3}$). A previous study showed that MSA concentrations in air masses with mixed influence from marine and biomass burning emissions are

higher than the concentrations measured from either source alone (Sorooshian et al., 2015). The results from the present study (i.e., more MSA measured in sets with biomass burning influence) in SE Asia again highlight the complexity of interactions between air masses with different sources and the accompanying changes in aerosol physiochemical properties.

4 Conclusions

This study sought to characterize influences of local and long-range transported aerosol to the Philippines during the Southwest Monsoon (SWM) season as well as the various synoptic- and local-scale conditions that facilitate and suppress long-range transport of aerosol. As a highly populated megacity, Metro Manila is the source of a large amount of urban, anthropogenic pollution. However, synoptic-scale weather, including the typical SWM flow and typhoons, can impact the transport of aerosol to and from Metro Manila. While previous work in a rural area in the northwest edge of the Philippines has identified seasonal aerosol transport patterns to the Philippines using $PM_{2.5}$ data (Bagtasa et al., 2018), the present study highlights case studies of in situ size-resolved aerosol measurements from Metro Manila to examine the potential for aerosol transport to impact this urban area as well.

For two of the sample sets with enhanced total water-soluble aerosol mass concentration, biomass burning aerosol transport from the Maritime Continent (MC) towards the Philippines was identified using air mass back trajectories and the NAAPS model. This transport followed a southwesterly flow pattern that is typical of this time of year (Fig. S2) and lends its name to the SWM season. Deep aerosol layers, extending from the surface to 3 km, were identified by CALIOP to the southwest of the Philippines. The influence on aerosol in Metro Manila was shown through enhancements in biomass burning tracer species (e.g., K, Rb) and increased concentration of organic aerosol. The challenges in satellite-based retrievals of biomass burning in the region (Reid et al., 2012, 2013) and the underestimation of fire activity in the region by these satellite retrievals (Reid et al., 2013) lead to unanswered questions about the amount and fate of biomass burning emissions in the MC and SE Asia. The ability to measure biomass burning signatures in a highly polluted, urban megacity such as Metro Manila and the evidence of long-range transport gathered through multiple methods and data sources (i.e., in situ measurements, models, and remote sensing) speak to the strong signature of biomass burning emissions in the region and the long-range transport pathways available for these emissions.

In contrast, transport of anthropogenic emissions from continental East Asia was identified on two occasions with high water-soluble aerosol mass concentrations, with one measured instance of long-range transport having been facilitated by the influence of a typhoon. In these cases, it is difficult to separate urban emissions between local and distant sources. However, the elevation of select tracer species (Ba, V, Pb, Mo, Sn) and the water-soluble organic aerosol characteristics for these two cases (i.e., high relative contribution of oxalate to the organic aerosol) indicated that long-range transported urban emissions could impact Metro Manila.

Finally, one low-aerosol-loading case was impacted by air masses traveling over the open ocean to the east of the Philippines. This case showed an enhanced fraction of supermicrometer aerosol and a very low concentration of water-soluble organic acids. Higher rain accumulation during this sample set, as opposed to the sample sets with the highest water-soluble aerosol concentrations, could have led to greater wet scavenging of aerosol. This case also had the lowest overall mass concentration of water-soluble organic species, a low percent contribution of oxalate to the water-soluble organics, and a high percent contribution of maleate. This result points to the relative importance of locally emitted species that have not yet undergone photochemical and aqueous processing mechanisms that lead to the degradation of longer-chain dicarboxylic acid species into oxalate.

These results have important implications for better understanding the aerosol budget in and around the Philippines and SE Asia via the identification of various tracer species (e.g., K and Rb for biomass burning) and the impacts of different long-range aerosol transport pathways. In addition, the mixing of different air mass types, resulting in changes in aerosol characteristics (e.g., enhanced oxalate in emissions from continental regions, enhanced MSA during periods of biomass burning influence), is a subject that requires more attention on a global basis. While this work has shown the influence of mixing biomass burning emissions and urban emissions, from both local and more distant urban centers, additional analysis at the study site has demonstrated the influences seen from the mixing of sea salt aerosol with other air masses (AzadiAghdam et al., 2019). As remote-sensing measurements in this region are notoriously difficult (e.g., Reid et al., 2009, 2013), in situ and model results lend vital data to address the questions surrounding characteristics of aerosol that are transported into and out of this highly populated region. Measurements from in situ airborne campaigns, such as CAMP^{2}Ex, can further address the changes in aerosol physicochemical characteristics that occur during long-range transport and aging in the atmosphere in the region.

Data availability. Ground-based size-resolved aerosol data from the Manila Observatory can be found at: https://doi.org/10.6084/m9.figshare.11861859 (Stahl et al., 2020).

Supplement. The supplement related to this article is available online at: https://doi.org/10.5194/acp-20-2387-2020-supplement.

Author contributions. MTC, MOC, JBS, RAB, ABM, CS, and AS designed the experiments, and all coauthors carried out some aspect of the data collection. MTC, RAB, CS, and AS conducted the data analysis and interpretation. RAB and AS prepared the manuscript with contributions from all coauthors.

Competing interests. The authors declare that they have no conflict of interest.

Acknowledgements. Rachel A. Braun acknowledges support from the ARCS Foundation. Melliza Templonuevo Cruz acknowledges support from the Philippine Department of Science and Technology's ASTHRD Program. Alexander B. MacDonald acknowledges support from the Mexican National Council of Science and Technology (CONACYT). We acknowledge Agilent Technologies for their support and Shane Snyder's laboratories for ICP-QQQ data.

Financial support. This research has been supported by the NASA (grant no. 80NSSC18K0148).

Review statement. This paper was edited by Joshua Fu and reviewed by three anonymous referees.

References

Aggarwal, S. G. and Kawamura, K.: Molecular distributions and stable carbon isotopic compositions of dicarboxylic acids and related compounds in aerosols from Sapporo, Japan: Implications for photochemical aging during long-range atmospheric transport, J. Geophys. Res.-Atmos., 113, D14301, https://doi.org/10.1029/2007jd009365, 2008.

Agrawal, H., Malloy, Q. G. J., Welch, W. A., Wayne Miller, J., and Cocker, D. R.: In-use gaseous and particulate matter emissions from a modern ocean going container vessel, Atmos. Environ., 42, 5504–5510, https://doi.org/10.1016/j.atmosenv.2008.02.053, 2008.

Akagi, S. K., Craven, J. S., Taylor, J. W., McMeeking, G. R., Yokelson, R. J., Burling, I. R., Urbanski, S. P., Wold, C. E., Seinfeld, J. H., Coe, H., Alvarado, M. J., and Weise, D. R.: Evolution of trace gases and particles emitted by a chaparral fire in California, Atmos. Chem. Phys., 12, 1397–1421, https://doi.org/10.5194/acp-12-1397-2012, 2012.

Alas, H. D., Müller, T., Birmili, W., Kecorius, S., Cambaliza, M. O., Simpas, J. B. B., Cayetano, M., Weinhold, K., Vallar, E., Galvez, M. C., and Wiedensohler, A.: Spatial Characterization of Black Carbon Mass Concentration in the Atmosphere of a Southeast Asian Megacity: An Air Quality Case Study for Metro Manila, Philippines, Aerosol Air Qual. Res., 18, 2301–2317, https://doi.org/10.4209/aaqr.2017.08.0281, 2018.

Allen, A. G., Nemitz, E., Shi, J. P., Harrison, R. M., and Greenwood, J. C.: Size distributions of trace metals in atmospheric aerosols in the United Kingdom, Atmos. Environ., 35, 4581–4591, https://doi.org/10.1016/S1352-2310(01)00190-X, 2001.

Amato, F., Pandolfi, M., Viana, M., Querol, X., Alastuey, A., and Moreno, T.: Spatial and chemical patterns of PM_{10} in road dust deposited in urban environment, Atmos. Environ., 43, 1650–1659, https://doi.org/10.1016/j.atmosenv.2008.12.009, 2009.

Andreae, M. O.: Soot Carbon and Excess Fine Potassium: Long-Range Transport of Combustion-Derived Aerosols, Science, 220, 1148, 10.1126/science.220.4602.1148, 1983.

Arimoto, R., Duce, R. A., Ray, B. J., Ellis Jr., W. G., Cullen, J. D., and Merrill, J. T.: Trace elements in the atmosphere over the North Atlantic, J. Geophys. Res.-Atmos., 100, 1199–1213, https://doi.org/10.1029/94jd02618, 1995.

Artaxo, P., Gerab, F., Yamasoe, M. A., and Martins, J. V.: Fine mode aerosol composition at three long-term atmospheric monitoring sites in the Amazon Basin, J. Geophys. Res.-Atmos., 99, 22857–22868, https://doi.org/10.1029/94jd01023, 1994.

Artaxo, P., Oyola, P., and Martinez, R.: Aerosol composition and source apportionment in Santiago de Chile, Nucl. Instrum. Meth. B, 150, 409–416, https://doi.org/10.1016/S0168-583X(98)01078-7, 1999.

Atwood, S. A., Reid, J. S., Kreidenweis, S. M., Cliff, S. S., Zhao, Y., Lin, N.-H., Tsay, S.-C., Chu, Y.-C., and Westphal, D. L.: Size resolved measurements of springtime aerosol particles over the northern South China Sea, Atmos. Environ., 78, 134–143, https://doi.org/10.1016/j.atmosenv.2012.11.024, 2013.

Atwood, S. A., Reid, J. S., Kreidenweis, S. M., Blake, D. R., Jonsson, H. H., Lagrosas, N. D., Xian, P., Reid, E. A., Sessions, W. R., and Simpas, J. B.: Size-resolved aerosol and cloud condensation nuclei (CCN) properties in the remote marine South China Sea – Part 1: Observations and source classification, Atmos. Chem. Phys., 17, 1105–1123, https://doi.org/10.5194/acp-17-1105-2017, 2017.

AzadiAghdam, M., Braun, R. A., Edwards, E.-L., Bañaga, P. A., Cruz, M. T., Betito, G., Cambaliza, M. O., Dadashazar, H., Lorenzo, G. R., Ma, L., MacDonald, A. B., Nguyen, P., Simpas, J. B., Stahl, C., and Sorooshian, A.: On the nature of sea salt aerosol at a coastal megacity: Insights from Manila, Philippines in Southeast Asia, Atmos. Environ., 216, 116922, https://doi.org/10.1016/j.atmosenv.2019.116922, 2019.

Bagtasa, G.: Effect of Synoptic Scale Weather Disturbance to Philippine Transboundary Oxone Pollution using WRF-CHEM, Int. J. Environ. Sci. Dev., 2, 402–405, https://doi.org/10.7763/IJESD.2011.V2.159, 2011.

Bagtasa, G., Cayetano, M. G., and Yuan, C.-S.: Seasonal variation and chemical characterization of $PM_{2.5}$ in northwestern Philippines, Atmos. Chem. Phys., 18, 4965–4980, https://doi.org/10.5194/acp-18-4965-2018, 2018.

Balla, D., Voutsa, D., and Samara, C.: Study of polar organic compounds in airborne particulate matter of a coastal urban city, Environ. Sci. Pollut. R., 25, 12191–12205, https://doi.org/10.1007/s11356-017-9993-2, 2018.

Bautista, A. T., Pabroa, P. C. B., Santos, F. L., Racho, J. M. D., and Quirit, L. L.: Carbonaceous particulate matter characterization in an urban and a rural site in the Philippines, Atmos. Pollut. Res., 5, 245–252, https://doi.org/10.5094/APR.2014.030, 2014.

Bovallius, A., Bucht, B., Roffey, R., and Anäs, P.: Long-range air transmission of bacteria, Appl. Environ. Microb., 35, 1231–1231, 1978.

Braun, R. A., Dadashazar, H., MacDonald, A. B., Aldhaif, A. M., Maudlin, L. C., Crosbie, E., Aghdam, M. A., Hossein Mardi, A., and Sorooshian, A.: Impact of Wildfire Emissions on Chloride and Bromide Depletion in Marine Aerosol Particles, Environ. Sci. Technol., 51, 9013–9021, https://doi.org/10.1021/acs.est.7b02039, 2017.

Brito, J., Freney, E., Dominutti, P., Borbon, A., Haslett, S. L., Batenburg, A. M., Colomb, A., Dupuy, R., Denjean, C., Burnet, F., Bourriane, T., Deroubaix, A., Sellegri, K., Borrmann, S., Coe, H., Flamant, C., Knippertz, P., and Schwarzenboeck, A.: Assessing the role of anthropogenic and biogenic sources on PM_1 over southern West Africa using aircraft measurements, Atmos. Chem. Phys., 18, 757–772, https://doi.org/10.5194/acp-18-757-2018, 2018.

Campbell, J. R., Reid, J. S., Westphal, D. L., Zhang, J., Tackett, J. L., Chew, B. N., Welton, E. J., Shimizu, A., Sugimoto, N., Aoki, K., and Winker, D. M.: Characterizing the vertical profile of aerosol particle extinction and linear depolarization over Southeast Asia and the Maritime Continent: The 2007–2009 view from CALIOP, Atmos. Res., 122, 520–543, https://doi.org/10.1016/j.atmosres.2012.05.007, 2013.

Cao, F., Zhang, S.-C., Kawamura, K., Liu, X., Yang, C., Xu, Z., Fan, M., Zhang, W., Bao, M., Chang, Y., Song, W., Liu, S., Lee, X., Li, J., Zhang, G., and Zhang, Y.-L.: Chemical characteristics of dicarboxylic acids and related organic compounds in $PM_{2.5}$ during biomass-burning and non-biomass-burning seasons at a rural site of Northeast China, Environ. Pollut., 231, 654–662, https://doi.org/10.1016/j.envpol.2017.08.045, 2017.

Cayanan, E. O., Chen, T.-C., Argete, J. C., Yen, M.-C., and Nilo, P. D.: The Effect of Tropical Cyclones on Southwest Monsoon Rainfall in the Philippines, J. Meteorol. Soc. Jpn., 89A, 123–139, https://doi.org/10.2151/jmsj.2011-A08, 2011.

Chang, L. T.-C., Tsai, J.-H., Lin, J.-M., Huang, Y.-S., and Chiang, H.-L.: Particulate matter and gaseous pollutants during a tropical storm and air pollution episode in Southern Taiwan, Atmos. Res., 99, 67–79, https://doi.org/10.1016/j.atmosres.2010.09.002, 2011.

Cheng, C., Li, M., Chan, C. K., Tong, H., Chen, C., Chen, D., Wu, D., Li, L., Wu, C., Cheng, P., Gao, W., Huang, Z., Li, X., Zhang, Z., Fu, Z., Bi, Y., and Zhou, Z.: Mixing state of oxalic acid containing particles in the rural area of Pearl River Delta, China: implications for the formation mechanism of oxalic acid, Atmos. Chem. Phys., 17, 9519–9533, https://doi.org/10.5194/acp-17-9519-2017, 2017.

Chow, J. C., Watson, J. G., Kuhns, H., Etyemezian, V., Lowenthal, D. H., Crow, D., Kohl, S. D., Engelbrecht, J. P., and Green, M. C.: Source profiles for industrial, mobile, and area sources in the Big Bend Regional Aerosol Visibility and Observational study, Chemosphere, 54, 185–208, https://doi.org/10.1016/j.chemosphere.2003.07.004, 2004.

Chuang, M.-T., Chang, S.-C., Lin, N.-H., Wang, J.-L., Sheu, G.-R., Chang, Y.-J., and Lee, C.-T.: Aerosol chemical properties and related pollutants measured in Dongsha Island in the northern South China Sea during 7-SEAS/Dongsha Experiment, Atmos. Environ., 78, 82–92, https://doi.org/10.1016/j.atmosenv.2012.05.014, 2013.

Crahan, K. K., Hegg, D., Covert, D. S., and Jonsson, H.: An exploration of aqueous oxalic acid production in the coastal marine atmosphere, Atmos. Environ., 38, 3757–3764, https://doi.org/10.1016/j.atmosenv.2004.04.009, 2004.

Cruz, F. T., Narisma, G. T., Villafuerte, M. Q., Cheng Chua, K. U., and Olaguera, L. M.: A climatological analysis of the southwest monsoon rainfall in the Philippines, Atmos. Res., 122, 609–616, https://doi.org/10.1016/j.atmosres.2012.06.010, 2013.

Cruz, M. T., Bañaga, P. A., Betito, G., Braun, R. A., Stahl, C., Aghdam, M. A., Cambaliza, M. O., Dadashazar, H., Hilario, M. R., Lorenzo, G. R., Ma, L., MacDonald, A. B., Pabroa, P. C., Yee, J. R., Simpas, J. B., and Sorooshian, A.: Size-resolved composition and morphology of particulate matter during the southwest monsoon in Metro Manila, Philippines, Atmos. Chem. Phys., 19, 10675–10696, https://doi.org/10.5194/acp-19-10675-2019, 2019.

Dave, P., Bhushan, M., and Venkataraman, C.: Aerosols cause intraseasonal short-term suppression of Indian monsoon rainfall, Sci. Rep.-UK, 7, 17347, https://doi.org/10.1038/s41598-017-17599-1, 2017.

Deshmukh, D. K., Deb, M. K., Hopke, P. K., and Tsai, Y. I.: Seasonal Characteristics of Water-Soluble Dicarboxylates Associated with PM_{10} in the Urban Atmosphere of Durg City, India, Aerosol Air Qual. Res., 12, 683–696, https://doi.org/10.4209/aaqr.2012.02.0040, 2012.

Deshmukh, D. K., Mozammel Haque, M., Kawamura, K., and Kim, Y.: Dicarboxylic acids, oxocarboxylic acids and α-dicarbonyls in fine aerosols over central Alaska: Implications for sources and atmospheric processes, Atmos. Res., 202, 128–139, https://doi.org/10.1016/j.atmosres.2017.11.003, 2018.

Duce, R. A., Liss, P. S., Merrill, J. T., Atlas, E. L., Buat-Menard, P., Hicks, B. B., Miller, J. M., Prospero, J. M., Arimoto, R., Church, T. M., Ellis, W., Galloway, J. N., Hansen, L., Jickells, T. D., Knap, A. H., Reinhardt, K. H., Schneider, B., Soudine, A., Tokos, J. J., Tsunogai, S., Wollast, R., and Zhou, M.: The atmospheric input of trace species to the world ocean, Global Biogeochem. Cy., 5, 193–259, https://doi.org/10.1029/91gb01778, 1991.

Echalar, F., Gaudichet, A., Cachier, H., and Artaxo, P.: Aerosol emissions by tropical forest and savanna biomass burning: Characteristic trace elements and fluxes, Geophys. Res. Lett., 22, 3039–3042, https://doi.org/10.1029/95gl03170, 1995.

Ervens, B.: Modeling the Processing of Aerosol and Trace Gases in Clouds and Fogs, Chem. Rev., 115, 4157–4198, https://doi.org/10.1021/cr5005887, 2015.

Ervens, B., Feingold, G., Frost, G. J., and Kreidenweis, S. M.: A modeling study of aqueous production of dicarboxylic acids: 1. Chemical pathways and speciated organic mass production, J. Geophys. Res.-Atmos., 109, D15205, https://doi.org/10.1029/2003jd004387, 2004.

Ervens, B., Sorooshian, A., Aldhaif, A. M., Shingler, T., Crosbie, E., Ziemba, L., Campuzano-Jost, P., Jimenez, J. L., and Wisthaler, A.: Is there an aerosol signature of chemical cloud processing?, Atmos. Chem. Phys., 18, 16099–16119, https://doi.org/10.5194/acp-18-16099-2018, 2018.

Falkovich, A. H., Graber, E. R., Schkolnik, G., Rudich, Y., Maenhaut, W., and Artaxo, P.: Low molecular weight organic acids in aerosol particles from Rondônia, Brazil, during the biomass-burning, transition and wet periods, Atmos. Chem. Phys., 5, 781–797, https://doi.org/10.5194/acp-5-781-2005, 2005.

Fang, G.-C., Lin, S.-J., Chang, S.-Y., and Chou, C.-C. K.: Effect of typhoon on atmospheric particulates in autumn in central Taiwan, Atmos. Environ., 43, 6039–6048, https://doi.org/10.1016/j.atmosenv.2009.08.033, 2009.

Farren, N. J., Dunmore, R. E., Mead, M. I., Mohd Nadzir, M. S., Samah, A. A., Phang, S.-M., Bandy, B. J., Sturges, W. T., and Hamilton, J. F.: Chemical characterisation of water-soluble ions in atmospheric particulate matter on the east coast of Peninsular Malaysia, Atmos. Chem. Phys., 19, 1537–1553, https://doi.org/10.5194/acp-19-1537-2019, 2019.

Flannigan, M., Cantin, A. S., de Groot, W. J., Wotton, M., Newbery, A., and Gowman, L. M.: Global wildland fire season severity in the 21st century, Forest Ecol. Manag., 294, 54–61, https://doi.org/10.1016/j.foreco.2012.10.022, 2013.

Flannigan, M. D., Krawchuk, M. A., de Groot, W. J., Wotton, B. M., and Gowman, L. M.: Implications of changing climate for global wildland fire, Int. J. Wildland Fire, 18, 483–507, https://doi.org/10.1071/WF08187, 2009.

Fujimori, T., Takigami, H., Agusa, T., Eguchi, A., Bekki, K., Yoshida, A., Terazono, A., and Ballesteros, F. C.: Impact of metals in surface matrices from formal and informal electronic-waste recycling around Metro Manila, the Philippines, and intra-Asian comparison, J. Hazard. Mater., 221–222, 139–146, https://doi.org/10.1016/j.jhazmat.2012.04.019, 2012.

Fung, Y. S. and Wong, L. W. Y.: Apportionment of air pollution sources by receptor models in Hong Kong, Atmos. Environ., 29, 2041–2048, https://doi.org/10.1016/1352-2310(94)00239-H, 1995.

Gadde, B., Bonnet, S., Menke, C., and Garivait, S.: Air pollutant emissions from rice straw open field burning in India, Thailand and the Philippines, Environ. Pollut., 157, 1554–1558, https://doi.org/10.1016/j.envpol.2009.01.004, 2009.

Ge, C., Wang, J., Reid, J. S., Posselt, D. J., Xian, P., and Hyer, E.: Mesoscale modeling of smoke transport from equatorial Southeast Asian Maritime Continent to the Philippines: First comparison of ensemble analysis with in situ observations, J. Geophys. Res.-Atmos., 122, 5380–5398, https://doi.org/10.1002/2016JD026241, 2017.

Gelaro, R., McCarty, W., Suárez, M. J., Todling, R., Molod, A., Takacs, L., Randles, C. A., Darmenov, A., Bosilovich, M. G., Reichle, R., Wargan, K., Coy, L., Cullather, R., Draper, C., Akella, S., Buchard, V., Conaty, A., Silva, A. M. d., Gu, W., Kim, G.-K., Koster, R., Lucchesi, R., Merkova, D., Nielsen, J. E., Partyka, G., Pawson, S., Putman, W., Rienecker, M., Schubert, S. D., Sienkiewicz, M., and Zhao, B.: The Modern-Era Retrospective Analysis for Research and Applications, Version 2 (MERRA-2), J. Climate, 30, 5419–5454, https://doi.org/10.1175/jcli-d-16-0758.1, 2017.

Global Modeling and Assimilation Office (GMAO): MERRA-2 inst3_3d_asm_Nv: 3d,3-Hourly,Instantaneous,Model-Level,Assimilation,Assimilated Meteorological Fields V5.12.4, Goddard Earth Sciences Data and Information Services Center (GES DISC), https://doi.org/10.5067/WWQSXQ8IVFW8, 2015a.

Global Modeling and Assimilation Office (GMAO): MERRA-2 tavg1_2d_rad_Nx: 2d,1-Hourly,Time-Averaged,Single-Level,Assimilation,Radiation Diagnostics V5.12.4, Goddard Earth Sciences Data and Information Services Center (GES DISC), https://doi.org/10.5067/Q9QMY5PBNV1T, 2015b.

Goldstein, A. H., Koven, C. D., Heald, C. L., and Fung, I. Y.: Biogenic carbon and anthropogenic pollutants combine to form a cooling haze over the southeastern United States, P. Natl. Acad. Sci. USA, 106, 8835–8840, https://doi.org/10.1073/pnas.0904128106, 2009.

Graf, H.-F., Yang, J., and Wagner, T. M.: Aerosol effects on clouds and precipitation during the 1997 smoke episode in Indonesia, Atmos. Chem. Phys., 9, 743–756, https://doi.org/10.5194/acp-9-743-2009, 2009.

Ho, K. F., Lee, S. C., Cao, J. J., Kawamura, K., Watanabe, T., Cheng, Y., and Chow, J. C.: Dicarboxylic acids, ketocarboxylic acids and dicarbonyls in the urban roadside area of Hong Kong, Atmos. Environ., 40, 3030–3040, https://doi.org/10.1016/j.atmosenv.2005.11.069, 2006.

Hogan, T. F., Liu, M., Ridout, J. A., Peng, M. S., Whitcomb, T. R., Ruston, B. C., Reynolds, C. A., Eckermann, S. D., Moskaitis, J. R., Baker, N. L., McCormack, J. P., Viner, K. C., McLay, J. G., Flatau, M. K., Xu, L., Chen, C., and Chang, S. W.: The Navy Global Environmental Model, Oceanography, 27, 116–125, https://doi.org/10.5670/oceanog.2014.73, 2014.

Hong, Y., Hsu, K.-L., Sorooshian, S., and Gao, X.: Precipitation Estimation from Remotely Sensed Imagery Using an Artificial Neural Network Cloud Classification System, J. Appl. Meteorol., 43, 1834–1853, https://doi.org/10.1175/jam2173.1, 2004.

Hoque, M. M. M., Kawamura, K., and Uematsu, M.: Spatio-temporal distributions of dicarboxylic acids, ω-oxocarboxylic acids, pyruvic acid, α-dicarbonyls and fatty acids in the marine aerosols from the North and South Pacific, Atmos. Res., 185, 158–168, https://doi.org/10.1016/j.atmosres.2016.10.022, 2017.

Hsieh, L.-Y., Kuo, S.-C., Chen, C.-L., and Tsai, Y. I.: Origin of low-molecular-weight dicarboxylic acids and their concentration and size distribution variation in suburban aerosol, Atmos. Environ., 41, 6648–6661, https://doi.org/10.1016/j.atmosenv.2007.04.014, 2007.

Hsieh, L.-Y., Chen, C.-L., Wan, M.-W., Tsai, C.-H., and Tsai, Y. I.: Speciation and temporal characterization of dicarboxylic acids in $PM_{2.5}$ during a PM episode and a period of non-episodic pollution, Atmos. Environ., 42, 6836–6850, https://doi.org/10.1016/j.atmosenv.2008.05.021, 2008.

Hyder, M., Genberg, J., Sandahl, M., Swietlicki, E., and Jönsson, J. Å.: Yearly trend of dicarboxylic acids in organic aerosols from south of Sweden and source attribution, Atmos. Environ., 57, 197–204, https://doi.org/10.1016/j.atmosenv.2012.04.027, 2012.

Jeong, C.-H., Wang, J. M., Hilker, N., Debosz, J., Sofowote, U., Su, Y., Noble, M., Healy, R. M., Munoz, T., Dabek-Zlotorzynska, E., Celo, V., White, L., Audette, C., Herod, D., and Evans, G. J.: Temporal and spatial variability of traffic-related $PM_{2.5}$ sources: Comparison of exhaust and non-exhaust emissions, Atmos. Environ., 198, 55–69, https://doi.org/10.1016/j.atmosenv.2018.10.038, 2019.

Juneng, L., Latif, M. T., and Tangang, F.: Factors influencing the variations of PM_{10} aerosol dust in Klang Valley, Malaysia during the summer, Atmos. Environ., 45, 4370–4378, https://doi.org/10.1016/j.atmosenv.2011.05.045, 2011.

Kawamura, K. and Ikushima, K.: Seasonal changes in the distribution of dicarboxylic acids in the urban atmosphere, Environ. Sci. Technol., 27, 2227–2235, https://doi.org/10.1021/es00047a033, 1993.

Kawamura, K. and Kaplan, I. R.: Motor exhaust emissions as a primary source for dicarboxylic acids in Los Angeles ambient air, Environ. Sci. Technol., 21, 105–110, https://doi.org/10.1021/es00155a014, 1987.

Kawamura, K. and Sakaguchi, F.: Molecular distributions of water soluble dicarboxylic acids in marine aerosols over the Pacific Ocean including tropics, J. Geophys. Res.-Atmos., 104, 3501–3509, https://doi.org/10.1029/1998jd100041, 1999.

Kawamura, K., Kasukabe, H., and Barrie, L. A.: Source and reaction pathways of dicarboxylic acids, ketoacids and dicarbonyls in arctic aerosols: One year of observations, Atmos. Environ., 30, 1709–1722, https://doi.org/10.1016/1352-2310(95)00395-9, 1996.

Kecorius, S., Madueño, L., Vallar, E., Alas, H., Betito, G., Birmili, W., Cambaliza, M. O., Catipay, G., Gonzaga-Cayetano, M., Galvez, M. C., Lorenzo, G., Müller, T., Simpas, J. B., Tamayo, E. G., and Wiedensohler, A.: Aerosol particle mixing state, refractory particle number size distributions and emission factors in a polluted urban environment: Case study of Metro Manila, Philippines, Atmos. Environ., 170, 169–183, https://doi.org/10.1016/j.atmosenv.2017.09.037, 2017.

Kim, E. and Hopke, P. K.: Source characterization of ambient fine particles at multiple sites in the Seattle area, Atmos. Environ., 42, 6047–6056, https://doi.org/10.1016/j.atmosenv.2008.03.032, 2008.

Kim, J. Y., Ghim, Y. S., Song, C. H., Yoon, S.-C., and Han, J. S.: Seasonal characteristics of air masses arriving at Gosan, Korea, using fine particle measurements between November 2001 and August 2003, J. Geophys. Res.-Atmos., 112, D07202, https://doi.org/10.1029/2005jd006946, 2007.

Kim Oanh, N. T., Upadhyay, N., Zhuang, Y. H., Hao, Z. P., Murthy, D. V. S., Lestari, P., Villarin, J. T., Chengchua, K., Co, H. X., Dung, N. T., and Lindgren, E. S.: Particulate air pollution in six Asian cities: Spatial and temporal distributions, and associated sources, Atmos. Environ., 40, 3367–3380, https://doi.org/10.1016/j.atmosenv.2006.01.050, 2006.

Kristiansen, N. I., Stohl, A., Olivié, D. J. L., Croft, B., Søvde, O. A., Klein, H., Christoudias, T., Kunkel, D., Leadbetter, S. J., Lee, Y. H., Zhang, K., Tsigaridis, K., Bergman, T., Evangeliou, N., Wang, H., Ma, P.-L., Easter, R. C., Rasch, P. J., Liu, X., Pitari, G., Di Genova, G., Zhao, S. Y., Balkanski, Y., Bauer, S. E., Faluvegi, G. S., Kokkola, H., Martin, R. V., Pierce, J. R., Schulz, M., Shindell, D., Tost, H., and Zhang, H.: Evaluation of observed and modelled aerosol lifetimes using radioactive tracers of opportunity and an ensemble of 19 global models, Atmos. Chem. Phys., 16, 3525–3561, https://doi.org/10.5194/acp-16-3525-2016, 2016.

Kumar, S., Aggarwal, S. G., Gupta, P. K., and Kawamura, K.: Investigation of the tracers for plastic-enriched waste burning aerosols, Atmos. Environ., 108, 49–58, https://doi.org/10.1016/j.atmosenv.2015.02.066, 2015.

Kunwar, B., Kawamura, K., Fujiwara, S., Fu, P., Miyazaki, Y., and Pokhrel, A.: Dicarboxylic acids, oxocarboxylic acids and α-dicarbonyls in atmospheric aerosols from Mt. Fuji, Japan: Implication for primary emission versus secondary formation, Atmos. Res., 221, 58–71, https://doi.org/10.1016/j.atmosres.2019.01.021, 2019.

Latif, M. T., Othman, M., Idris, N., Juneng, L., Abdullah, A. M., Hamzah, W. P., Khan, M. F., Nik Sulaiman, N. M., Jewaratnam, J., Aghamohammadi, N., Sahani, M., Xiang, C. J., Ahamad, F., Amil, N., Darus, M., Varkkey, H., Tangang, F., and Jaafar, A. B.: Impact of regional haze towards air quality in Malaysia: A review, Atmos. Environ., 177, 28–44, https://doi.org/10.1016/j.atmosenv.2018.01.002, 2018.

Li, X.-d., Yang, Z., Fu, P., Yu, J., Lang, Y.-c., Liu, D., Ono, K., and Kawamura, K.: High abundances of dicarboxylic acids, oxocarboxylic acids, and α-dicarbonyls in fine aerosols ($PM_{2.5}$) in Chengdu, China during wintertime haze pollution, Environ. Sci. Pollut. R., 22, 12902–12918, https://doi.org/10.1007/s11356-015-4548-x, 2015.

Lin, C.-C., Chen, S.-J., Huang, K.-L., Hwang, W.-I., Chang-Chien, G.-P., and Lin, W.-Y.: Characteristics of Metals in Nano/Ultrafine/Fine/Coarse Particles Collected Beside a Heavily Trafficked Road, Environ. Sci. Technol., 39, 8113–8122, https://doi.org/10.1021/es048182a, 2005.

Lin, C.-Y., Hsu, H.-m., Lee, Y. H., Kuo, C. H., Sheng, Y.-F., and Chu, D. A.: A new transport mechanism of biomass burning from Indochina as identified by modeling studies, Atmos. Chem. Phys., 9, 7901–7911, https://doi.org/10.5194/acp-9-7901-2009, 2009.

Lin, I. I., Chen, J.-P., Wong, G. T. F., Huang, C.-W., and Lien, C.-C.: Aerosol input to the South China Sea: Results from the MODerate Resolution Imaging Spectro-radiometer, the Quick Scatterometer, and the Measurements of Pollution in the Troposphere Sensor, Deep-Sea Res. Pt. II, 54, 1589–1601, https://doi.org/10.1016/j.dsr2.2007.05.013, 2007.

Lindqvist, O., Johansson, K., Bringmark, L., Timm, B., Aastrup, M., Andersson, A., Hovsenius, G., Håkanson, L., Iverfeldt, Å., and Meili, M.: Mercury in the Swedish environment – Recent research on causes, consequences and corrective methods, Water Air Soil Pollut., 55, xi–xv, https://doi.org/10.1007/bf00542429, 1991.

Liu, W., Han, Y., Yin, Y., Duan, J., Gong, J., Liu, Z., and Xu, W.: An aerosol air pollution episode affected by binary typhoons in east and central China, Atmos. Pollut. Res., 9, 634–642, https://doi.org/10.1016/j.apr.2018.01.005, 2018.

Liu, Y., Cai, W., Sun, C., Song, H., Cobb, K. M., Li, J., Leavitt, S. W., Wu, L., Cai, Q., Liu, R., Ng, B., Cherubini, P., Büentgen, U., Song, Y., Wang, G., Lei, Y., Yan, L., Li, Q., Ma, Y., Fang, C., Sun, J., Li, X., Chen, D., and Linderholm, H. W.: Anthropogenic aerosols cause recent pronounced weakening of Asian Summer Monsoon relative to last four centuries, Geophys. Res. Lett., 46, 5469–5479, https://doi.org/10.1029/2019gl082497, 2019.

Lu, C.-C., Yuan, C.-S., and Li, T.-C.: How Aeolian Dust Deteriorate Ambient Particulate Air Quality along an Expansive River Valley in Southern Taiwan? A Case Study of Typhoon Doksuri, Aerosol Air Qual. Res., 17, 2181–2196, https://doi.org/10.4209/aaqr.2017.08.0257, 2017.

Lynch, P., Reid, J. S., Westphal, D. L., Zhang, J., Hogan, T. F., Hyer, E. J., Curtis, C. A., Hegg, D. A., Shi, Y., Campbell, J. R., Rubin, J. I., Sessions, W. R., Turk, F. J., and Walker, A. L.: An 11-year global gridded aerosol optical thickness reanalysis (v1.0) for atmospheric and climate sciences, Geosci. Model Dev., 9, 1489–1522, https://doi.org/10.5194/gmd-9-1489-2016, 2016.

Lyons, W. A., Dooley, J. C., and Whitby, K. T.: Satellite detection of long-range pollution transport and sulfate aerosol hazes, Atmos. Environ., 12, 621–631, https://doi.org/10.1016/0004-6981(78)90242-1, 1978.

Ma, L., Dadashazar, H., Braun, R. A., MacDonald, A. B., Aghdam, M. A., Maudlin, L. C., and Sorooshian, A.: Size-resolved Characteristics of Water-Soluble Particulate Elements in a Coastal Area: Source Identification, Influence of Wildfires, and Diurnal Variability, Atmos. Environ., 206, 72–84, https://doi.org/10.1016/j.atmosenv.2019.02.045, 2019.

Maenhaut, W., Salma, I., Cafmeyer, J., Annegarn, H. J., and Andreae, M. O.: Regional atmospheric aerosol composition and sources in the eastern Transvaal, South Africa, and impact of biomass burning, J. Geophys. Res.-Atmos., 101, 23631–23650, https://doi.org/10.1029/95jd02930, 1996.

Maki, T., Lee, K. C., Kawai, K., Onishi, K., Hong, C. S., Kurosaki, Y., Shinoda, M., Kai, K., Iwasaka, Y., Archer, S. D. J., Lacap-Bugler, D. C., Hasegawa, H., and Pointing, S. B.: Aeolian dispersal of bacteria associated with desert dust and anthropogenic particles over continental and oceanic surfaces, J. Geophys. Res.-Atmos., 124, 5579–5588, https://doi.org/10.1029/2018jd029597, 2019.

Mamoudou, I., Zhang, F., Chen, Q., Wang, P., and Chen, Y.: Characteristics of $PM_{2.5}$ from ship emissions and their impacts on the ambient air: A case study in Yangshan Harbor, Shanghai, Sci. Total Environ., 640–641, 207–216, https://doi.org/10.1016/j.scitotenv.2018.05.261, 2018.

Marple, V., Olson, B., Romay, F., Hudak, G., Geerts, S. M., and Lundgren, D.: Second Generation Micro-Orifice Uniform Deposit Impactor, 120 MOUDI-II: Design, Evaluation, and Application to Long-Term Ambient Sampling, Aerosol Sci. Tech., 48, 427–433, https://doi.org/10.1080/02786826.2014.884274, 2014.

Maudlin, L. C., Wang, Z., Jonsson, H. H., and Sorooshian, A.: Impact of wildfires on size-resolved aerosol composition at a coastal California site, Atmos. Environ., 119, 59–68, https://doi.org/10.1016/j.atmosenv.2015.08.039, 2015.

Mosher, B. W. and Duce, R. A.: A global atmospheric selenium budget, J. Geophys. Res.-Atmos., 92, 13289–13298, https://doi.org/10.1029/JD092iD11p13289, 1987.

Nguyen, P., Sellars, S., Thorstensen, A., Tao, Y., Ashouri, H., Braithwaite, D., Hsu, K., and Sorooshian, S.: Satellites Track Precipitation of Super Typhoon Haiyan, Eos Trans. AGU, 95, 133–135, https://doi.org/10.1002/2014eo160002, 2014.

Nguyen, P., Shearer, E. J., Tran, H., Ombadi, M., Hayatbini, N., Palacios, T., Huynh, P., Braithwaite, D., Updegraff, G., Hsu, K., Kuligowski, B., Logan, W. S., and Sorooshian, S.: The CHRS Data Portal, an easily accessible public repository for PERSIANN global satellite precipitation data, Scientific Data, 6, 180296, https://doi.org/10.1038/sdata.2018.296, 2019.

Nirmalkar, J., Deshmukh, D. K., Deb, M. K., Tsai, Y. I., and Sopajaree, K.: Mass loading and episodic variation of molecular markers in $PM_{2.5}$ aerosols over a rural area in eastern central India, Atmos. Environ., 117, 41–50, https://doi.org/10.1016/j.atmosenv.2015.07.003, 2015.

Nordø, J.: Long range transport of air pollutants in Europe and acid precipitation in Norway, Water Air Soil Pollut., 6, 199–217, https://doi.org/10.1007/bf00182865, 1976.

Pakkanen, T. A., Loukkola, K., Korhonen, C. H., Aurela, M., Mäkelä, T., Hillamo, R. E., Aarnio, P., Koskentalo, T., Kousa, A., and Maenhaut, W.: Sources and chemical composition of atmospheric fine and coarse particles in the Helsinki area, Atmos. Environ., 35, 5381–5391, https://doi.org/10.1016/S1352-2310(01)00307-7, 2001.

Pakkanen, T. A., Kerminen, V.-M., Loukkola, K., Hillamo, R. E., Aarnio, P., Koskentalo, T., and Maenhaut, W.: Size distributions of mass and chemical components in street-level and rooftop PM_1 particles in Helsinki, Atmos. Environ., 37, 1673–1690, https://doi.org/10.1016/S1352-2310(03)00011-6, 2003.

Pandolfi, M., Gonzalez-Castanedo, Y., Alastuey, A., de la Rosa, J. D., Mantilla, E., de la Campa, A. S., Querol, X., Pey, J., Amato, F., and Moreno, T.: Source apportionment of PM_{10} and $PM_{2.5}$ at multiple sites in the strait of Gibraltar by PMF: impact of shipping emissions, Environ. Sci. Pollut. R., 18, 260–269, https://doi.org/10.1007/s11356-010-0373-4, 2011.

Philippine Statistics Authority: available at: https://psa.gov.ph/content/population-national-capital-region-based-2015-census-population-0, last access: 24 February 2020.

Querol, X., Alastuey, A., Moreno, T., Viana, M. M., Castillo, S., Pey, J., Rodríguez, S., Artiñano, B., Salvador, P., Sánchez, M., Garcia Dos Santos, S., Herce Garraleta, M. D., Fernandez-Patier, R., Moreno-Grau, S., Negral, L., Minguillón, M. C., Monfort, E., Sanz, M. J., Palomo-Marín, R., Pinilla-Gil, E., Cuevas, E., de la Rosa, J., and Sánchez de la Campa, A.: Spatial and temporal variations in airborne particulate matter (PM_{10} and $PM_{2.5}$) across Spain 1999–2005, Atmos. Environ., 42, 3964–3979, https://doi.org/10.1016/j.atmosenv.2006.10.071, 2008.

Ray, J. and McDow, S. R.: Dicarboxylic acid concentration trends and sampling artifacts, Atmos. Environ., 39, 7906–7919, https://doi.org/10.1016/j.atmosenv.2005.09.024, 2005.

Reid, J. S., Hyer, E. J., Prins, E. M., Westphal, D. L., Zhang, J., Wang, J., Christopher, S. A., Curtis, C. A., Schmidt, C. C., Eleuterio, D. P., Richardson, K. A., and Hoffman, J. P.: Global Monitoring and Forecasting of Biomass-Burning Smoke: Description of and Lessons From the Fire Locating and Modeling of Burning Emissions (FLAMBE) Program, IEEE J. Sel. Top. Appl., 2, 144–162, https://doi.org/10.1109/jstars.2009.2027443, 2009.

Reid, J. S., Xian, P., Hyer, E. J., Flatau, M. K., Ramirez, E. M., Turk, F. J., Sampson, C. R., Zhang, C., Fukada, E. M., and Maloney, E. D.: Multi-scale meteorological conceptual analysis of observed active fire hotspot activity and smoke optical depth in the Maritime Continent, Atmos. Chem. Phys., 12, 2117–2147, https://doi.org/10.5194/acp-12-2117-2012, 2012.

Reid, J. S., Hyer, E. J., Johnson, R. S., Holben, B. N., Yokelson, R. J., Zhang, J., Campbell, J. R., Christopher, S. A., Di Girolamo, L., Giglio, L., Holz, R. E., Kearney, C., Miettinen, J., Reid, E. A., Turk, F. J., Wang, J., Xian, P., Zhao, G., Balasubramanian, R., Chew, B. N., Janjai, S., Lagrosas, N., Lestari, P., Lin, N.-H., Mahmud, M., Nguyen, A. X., Norris, B., Oanh, N. T. K., Oo, M., Salinas, S. V., Welton, E. J., and Liew, S. C.: Observing and understanding the Southeast Asian aerosol system by remote sensing: An initial review and analysis for the Seven Southeast Asian Studies (7SEAS) program, Atmos. Res., 122, 403–468, https://doi.org/10.1016/j.atmosres.2012.06.005, 2013.

Reid, J. S., Lagrosas, N. D., Jonsson, H. H., Reid, E. A., Sessions, W. R., Simpas, J. B., Uy, S. N., Boyd, T. J., Atwood, S. A., Blake, D. R., Campbell, J. R., Cliff, S. S., Holben, B. N., Holz, R. E., Hyer, E. J., Lynch, P., Meinardi, S., Posselt, D. J., Richardson, K. A., Salinas, S. V., Smirnov, A., Wang, Q., Yu, L., and Zhang, J.: Observations of the temporal variability in aerosol properties and their relationships to meteorology in the summer monsoonal South China Sea/East Sea: the scale-dependent role of mon-

soonal flows, the Madden–Julian Oscillation, tropical cyclones, squall lines and cold pools, Atmos. Chem. Phys., 15, 1745–1768, https://doi.org/10.5194/acp-15-1745-2015, 2015.

Reid, J. S., Xian, P., Holben, B. N., Hyer, E. J., Reid, E. A., Salinas, S. V., Zhang, J., Campbell, J. R., Chew, B. N., Holz, R. E., Kuciauskas, A. P., Lagrosas, N., Posselt, D. J., Sampson, C. R., Walker, A. L., Welton, E. J., and Zhang, C.: Aerosol meteorology of the Maritime Continent for the 2012 7SEAS southwest monsoon intensive study – Part 1: regional-scale phenomena, Atmos. Chem. Phys., 16, 14041–14056, https://doi.org/10.5194/acp-16-14041-2016, 2016a.

Reid, J. S., Lagrosas, N. D., Jonsson, H. H., Reid, E. A., Atwood, S. A., Boyd, T. J., Ghate, V. P., Xian, P., Posselt, D. J., Simpas, J. B., Uy, S. N., Zaiger, K., Blake, D. R., Bucholtz, A., Campbell, J. R., Chew, B. N., Cliff, S. S., Holben, B. N., Holz, R. E., Hyer, E. J., Kreidenweis, S. M., Kuciauskas, A. P., Lolli, S., Oo, M., Perry, K. D., Salinas, S. V., Sessions, W. R., Smirnov, A., Walker, A. L., Wang, Q., Yu, L., Zhang, J., and Zhao, Y.: Aerosol meteorology of Maritime Continent for the 2012 7SEAS southwest monsoon intensive study – Part 2: Philippine receptor observations of fine-scale aerosol behavior, Atmos. Chem. Phys., 16, 14057–14078, https://doi.org/10.5194/acp-16-14057-2016, 2016b.

Ross, A. D., Holz, R. E., Quinn, G., Reid, J. S., Xian, P., Turk, F. J., and Posselt, D. J.: Exploring the first aerosol indirect effect over Southeast Asia using a 10-year collocated MODIS, CALIOP, and model dataset, Atmos. Chem. Phys., 18, 12747–12764, https://doi.org/10.5194/acp-18-12747-2018, 2018.

Satsumabayashi, H., Kurita, H., Yokouchi, Y., and Ueda, H.: Photochemical formation of particulate dicarboxylic acids under long-range transport in central Japan, Atmos. Environ. A-Gen., 24, 1443–1450, https://doi.org/10.1016/0960-1686(90)90053-P, 1990.

Schlosser, J. S., Braun, R. A., Bradley, T., Dadashazar, H., MacDonald, A. B., Aldhaif, A. A., Aghdam, M. A., Mardi, A. H., Xian, P., and Sorooshian, A.: Analysis of aerosol composition data for western United States wildfires between 2005 and 2015: Dust emissions, chloride depletion, and most enhanced aerosol constituents, J. Geophys. Res.-Atmos., 122, 8951–8966, https://doi.org/10.1002/2017jd026547, 2017.

Simpas, J., Lorenzo, G., and Cruz, M. T.: Monitoring Particulate Matter Levels and Composition for Source Apportionment Study in Metro Manila, Philippines, in: Improving Air Quality in Asian Developing Countries: Compilation of Research Findings, edited by: Kim Oanh, N. T., NARENCA, Vietnam Publishing House of Natural Resources, Environment and Cartography, Vietnam, 239–261, 2014.

Singh, M., Jaques, P. A., and Sioutas, C.: Size distribution and diurnal characteristics of particle-bound metals in source and receptor sites of the Los Angeles Basin, Atmos. Environ., 36, 1675–1689, https://doi.org/10.1016/S1352-2310(02)00166-8, 2002.

Song, J., Zhao, Y., Zhang, Y., Fu, P., Zheng, L., Yuan, Q., Wang, S., Huang, X., Xu, W., Cao, Z., Gromov, S., and Lai, S.: Influence of biomass burning on atmospheric aerosols over the western South China Sea: Insights from ions, carbonaceous fractions and stable carbon isotope ratios, Environ. Pollut., 242, 1800–1809, https://doi.org/10.1016/j.envpol.2018.07.088, 2018.

Song, X.-H., Polissar, A. V., and Hopke, P. K.: Sources of fine particle composition in the northeastern US, Atmos. Environ., 35, 5277–5286, https://doi.org/10.1016/S1352-2310(01)00338-7, 2001.

Sorooshian, A., Varutbangkul, V., Brechtel, F. J., Ervens, B., Feingold, G., Bahreini, R., Murphy, S. M., Holloway, J. S., Atlas, E. L., Buzorius, G., Jonsson, H., Flagan, R. C., and Seinfeld, J. H.: Oxalic acid in clear and cloudy atmospheres: Analysis of data from International Consortium for Atmospheric Research on Transport and Transformation 2004, J. Geophys. Res.-Atmos., 111, D23S45, https://doi.org/10.1029/2005jd006880, 2006.

Sorooshian, A., Ng, N. L., Chan, A. W. H., Feingold, G., Flagan, R. C., and Seinfeld, J. H.: Particulate organic acids and overall water-soluble aerosol composition measurements from the 2006 Gulf of Mexico Atmospheric Composition and Climate Study (GoMACCS), J. Geophys. Res.-Atmos., 112, D13201, https://doi.org/10.1029/2007jd008537, 2007a.

Sorooshian, A., Lu, M.-L., Brechtel, F. J., Jonsson, H., Feingold, G., Flagan, R. C., and Seinfeld, J. H.: On the Source of Organic Acid Aerosol Layers above Clouds, Environ. Sci. Technol., 41, 4647–4654, https://doi.org/10.1021/es0630442, 2007b.

Sorooshian, A., Crosbie, E., Maudlin, L. C., Youn, J.-S., Wang, Z., Shingler, T., Ortega, A. M., Hersey, S., and Woods, R. K.: Surface and airborne measurements of organosulfur and methanesulfonate over the western United States and coastal areas, J. Geophys. Res.-Atmos., 120, 8535–8548, https://doi.org/10.1002/2015jd023822, 2015.

Stahl, C., Cruz, M. T., Bañaga, P. A., Betito, G., Braun, R. A., Aghdam, M. A., Cambaliza, M. O., Lorenzo, G. R., MacDonald, A. B., Pabroa, P. C., Yee, J. R., Simpas, J. B., and Sorooshian, A.: An Annual Time Series of Weekly Size-Resolved Aerosol Properties in the Megacity of Metro Manila, Philippines, figshare, https://doi.org/10.6084/m9.figshare.11861859, 2020.

Stein, A. F., Draxler, R. R., Rolph, G. D., Stunder, B. J. B., Cohen, M. D., and Ngan, F.: NOAA's HYSPLIT Atmospheric Transport and Dispersion Modeling System, B. Am. Meteorol. Soc., 96, 2059–2077, https://doi.org/10.1175/bams-d-14-00110.1, 2015.

Sternbeck, J., Sjödin, Å., and Andréasson, K.: Metal emissions from road traffic and the influence of resuspension–results from two tunnel studies, Atmos. Environ., 36, 4735–4744, https://doi.org/10.1016/S1352-2310(02)00561-7, 2002.

Thepnuan, D., Chantara, S., Lee, C.-T., Lin, N.-H., and Tsai, Y. I.: Molecular markers for biomass burning associated with the characterization of $PM_{2.5}$ and component sources during dry season haze episodes in Upper South East Asia, Sci. Total Environ., 658, 708–722, https://doi.org/10.1016/j.scitotenv.2018.12.201, 2019.

Thurston, G. D. and Spengler, J. D.: A quantitative assessment of source contributions to inhalable particulate matter pollution in metropolitan Boston, Atmos. Environ., 19, 9–25, https://doi.org/10.1016/0004-6981(85)90132-5, 1985.

Vaughan, M. A., Young, S. A., Winker, D. M., Powell, K. A., Omar, A. H., Liu, Z., Hu, Y., and Hostetler, C. A.: Fully automated analysis of space-based lidar data: an overview of the CALIPSO retrieval algorithms and data products, in: Proceedings of SPIE Volume 5575, Laser Radar Techniques for Atmospheric Sensing, Maspalomas, Canary Islands, Spain, 4 November 2004, 16–30, https://doi.org/10.1117/12.572024, 2004.

Wang, H. and Shooter, D.: Low molecular weight dicarboxylic acids in PM_{10} in a city with intensive solid fuel burning, Chemosphere, 56, 725–733, https://doi.org/10.1016/j.chemosphere.2004.04.030, 2004.

Wang, J., Ge, C., Yang, Z., Hyer, E. J., Reid, J. S., Chew, B.-N., Mahmud, M., Zhang, Y., and Zhang, M.: Mesoscale modeling of smoke transport over the Southeast Asian Maritime Continent: Interplay of sea breeze, trade wind, typhoon, and topography, Atmos. Res., 122, 486–503, https://doi.org/10.1016/j.atmosres.2012.05.009, 2013.

Wang, S.-H., Tsay, S.-C., Lin, N.-H., Hsu, N. C., Bell, S. W., Li, C., Ji, Q., Jeong, M.-J., Hansell, R. A., Welton, E. J., Holben, B. N., Sheu, G.-R., Chu, Y.-C., Chang, S.-C., Liu, J.-J., and Chiang, W.-L.: First detailed observations of long-range transported dust over the northern South China Sea, Atmos. Environ., 45, 4804–4808, https://doi.org/10.1016/j.atmosenv.2011.04.077, 2011.

Weber, R. J., Sullivan, A. P., Peltier, R. E., Russell, A., Yan, B., Zheng, M., de Gouw, J., Warneke, C., Brock, C., Holloway, J. S., Atlas, E. L., and Edgerton, E.: A study of secondary organic aerosol formation in the anthropogenic-influenced southeastern United States, J. Geophys. Res.-Atmos., 112, D13302, https://doi.org/10.1029/2007jd008408, 2007.

Wen, H. and Carignan, J.: Reviews on atmospheric selenium: Emissions, speciation and fate, Atmos. Environ., 41, 7151–7165, https://doi.org/10.1016/j.atmosenv.2007.07.035, 2007.

Winker, D. M., Vaughan, M. A., Omar, A., Hu, Y., Powell, K. A., Liu, Z., Hunt, W. H., and Young, S. A.: Overview of the CALIPSO Mission and CALIOP Data Processing Algorithms, J. Atmos. Ocean. Tech., 26, 2310–2323, https://doi.org/10.1175/2009jtecha1281.1, 2009.

Wonaschuetz, A., Sorooshian, A., Ervens, B., Chuang, P. Y., Feingold, G., Murphy, S. M., de Gouw, J., Warneke, C., and Jonsson, H. H.: Aerosol and gas re-distribution by shallow cumulus clouds: An investigation using airborne measurements, J. Geophys. Res.-Atmos., 117, D17202, https://doi.org/10.1029/2012jd018089, 2012.

Xian, P., Reid, J. S., Atwood, S. A., Johnson, R. S., Hyer, E. J., Westphal, D. L., and Sessions, W.: Smoke aerosol transport patterns over the Maritime Continent, Atmos. Res., 122, 469–485, https://doi.org/10.1016/j.atmosres.2012.05.006, 2013.

Xu, J., Zhang, J., Liu, J., Yi, K., Xiang, S., Hu, X., Wang, Y., Tao, S., and Ban-Weiss, G.: Influence of cloud microphysical processes on black carbon wet removal, global distributions, and radiative forcing, Atmos. Chem. Phys., 19, 1587–1603, https://doi.org/10.5194/acp-19-1587-2019, 2019.

Yamasoe, M. A., Artaxo, P., Miguel, A. H., and Allen, A. G.: Chemical composition of aerosol particles from direct emissions of vegetation fires in the Amazon Basin: water-soluble species and trace elements, Atmos. Environ., 34, 1641–1653, https://doi.org/10.1016/S1352-2310(99)00329-5, 2000.

Yan, J., Chen, L., Lin, Q., Zhao, S., and Zhang, M.: Effect of typhoon on atmospheric aerosol particle pollutants accumulation over Xiamen, China, Chemosphere, 159, 244–255, https://doi.org/10.1016/j.chemosphere.2016.06.006, 2016.

Yao, X., Fang, M., Chan, C. K., Ho, K. F., and Lee, S. C.: Characterization of dicarboxylic acids in $PM_{2.5}$ in Hong Kong, Atmos. Environ., 38, 963–970, https://doi.org/10.1016/j.atmosenv.2003.10.048, 2004.

Yokelson, R. J., Crounse, J. D., DeCarlo, P. F., Karl, T., Urbanski, S., Atlas, E., Campos, T., Shinozuka, Y., Kapustin, V., Clarke, A. D., Weinheimer, A., Knapp, D. J., Montzka, D. D., Holloway, J., Weibring, P., Flocke, F., Zheng, W., Toohey, D., Wennberg, P. O., Wiedinmyer, C., Mauldin, L., Fried, A., Richter, D., Walega, J., Jimenez, J. L., Adachi, K., Buseck, P. R., Hall, S. R., and Shetter, R.: Emissions from biomass burning in the Yucatan, Atmos. Chem. Phys., 9, 5785–5812, https://doi.org/10.5194/acp-9-5785-2009, 2009.

Zhang, Y.-N., Zhang, Z.-S., Chan, C.-Y., Engling, G., Sang, X.-F., Shi, S., and Wang, X.-M.: Levoglucosan and carbonaceous species in the background aerosol of coastal southeast China: case study on transport of biomass burning smoke from the Philippines, Environ. Sci. Pollut. R., 19, 244–255, https://doi.org/10.1007/s11356-011-0548-7, 2012.

Zhao, X., Wang, X., Ding, X., He, Q., Zhang, Z., Liu, T., Fu, X., Gao, B., Wang, Y., Zhang, Y., Deng, X., and Wu, D.: Compositions and sources of organic acids in fine particles ($PM_{2.5}$) over the Pearl River Delta region, south China, J. Environ. Sci., 26, 110–121, https://doi.org/10.1016/S1001-0742(13)60386-1, 2014.